



Marianne Liebi– Material Science at Large Scale Facilities

Small-angle scattering (SAXS/SANS)

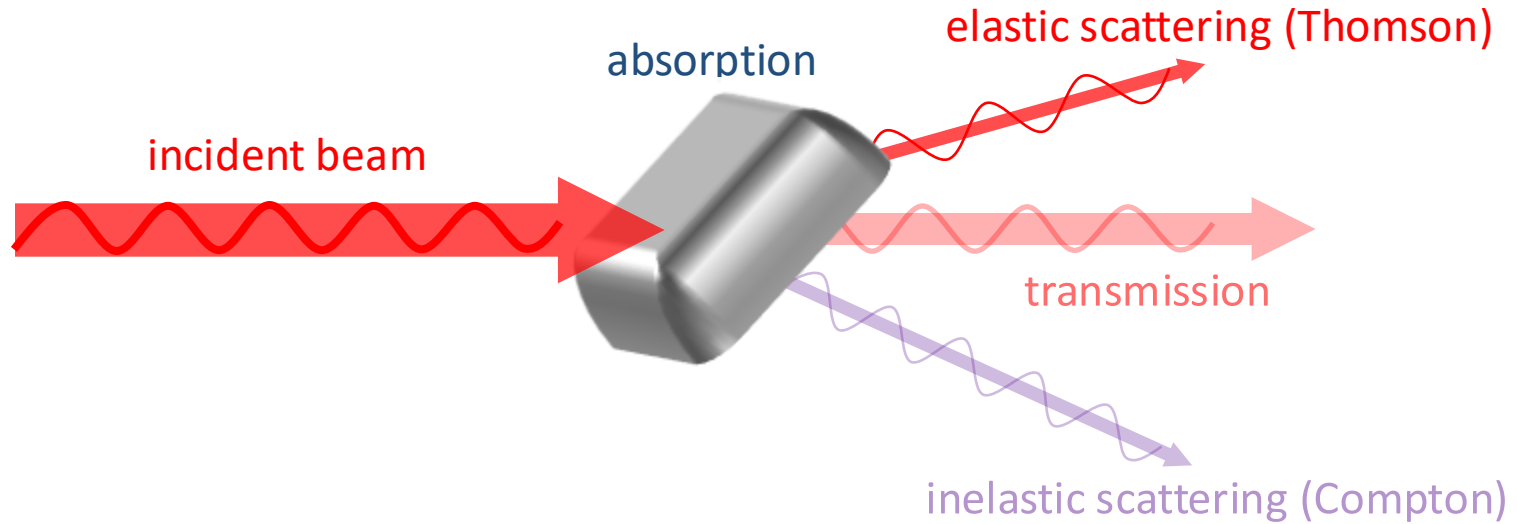
EPFL Master Course 2025 MSE435

Course program

Dates	Content	Lecturer
08.09.25	Introduction, sources, beamlines, detectors	Steven Van Petegem
15.09.25	Excursion to PSI	Marianne Liebi
22.09.25	Holiday	
29.09.25	Interaction with matter	Steven Van Petegem
06.10.25	Fluorescence	Marianne Liebi
13.10.25	X-ray absorption spectroscopy	Marianne Liebi
20.10.25	Break	
27.10.25	Diffraction I	Steven Van Petegem
03.11.25	Small angle scattering	Marianne Liebi
10.11.25	Diffraction II	Steven Van Petegem
17.11.25	Phase contrast / Tomography	Steven Van Petegem
24.11.25	Coherent imaging	Marianne Liebi
01.12.25	Neutron imaging	Steven Van Petegem
08.12.25	PEEM / Magnetic scattering	Steven Van Petegem
15.12.25	Case study presentations	Steven Van Petegem / Marianne Liebi

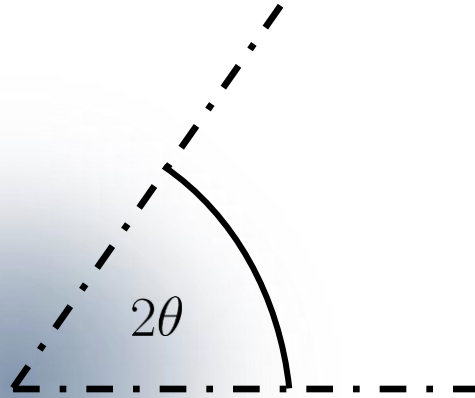
Interaction of X-rays with matter

interaction with electrons

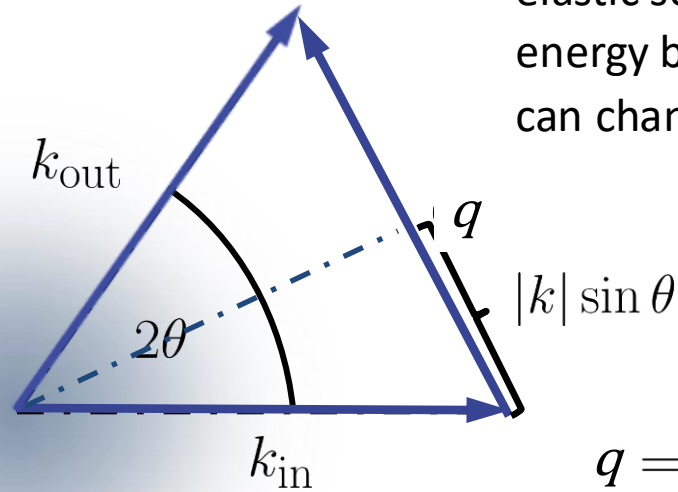


Elastic scattering of photons

elastic scattering: no loss in photon energy but direction or of the photon can change: scattering angle 2θ



Elastic scattering of photons



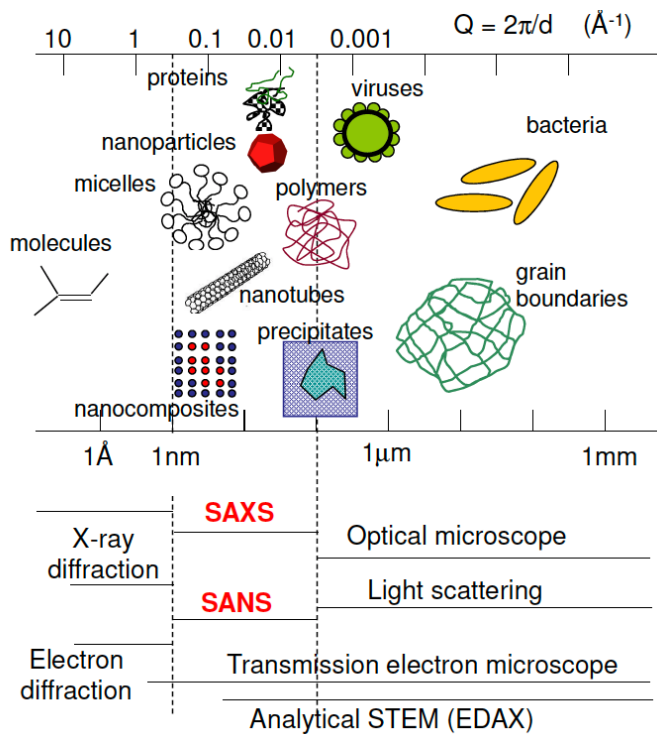
elastic scattering: no loss in photon energy but direction or of the photon can change: scattering angle 2θ

$$q = 2|k| \sin \theta = (4\pi/\lambda) \sin \theta$$

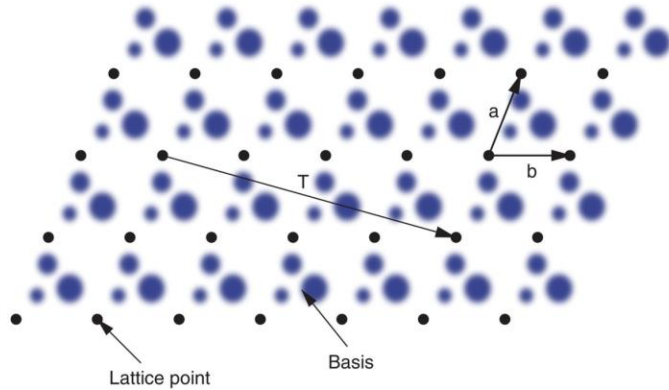
wave vector $k = 2\pi/\lambda$

scattering vector $\mathbf{q} = \mathbf{k}_{in} - \mathbf{k}_{out}$

Size range comparison

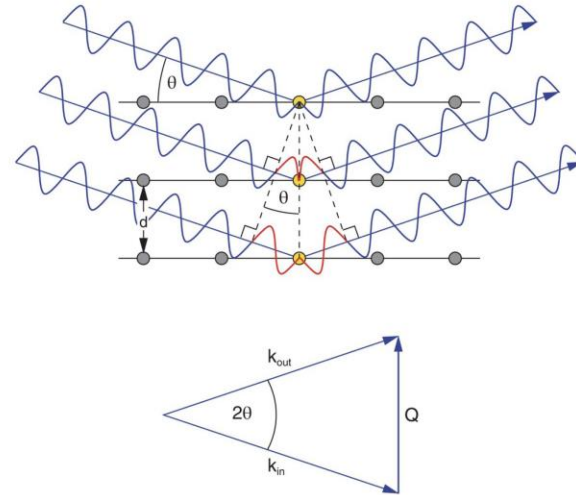


Diffraction on crystals and Bragg's law



If one derives it from an analogy with the slits, the distance between the atoms is the grating distance and the size of the atoms is the width of the slit.

Bragg's law

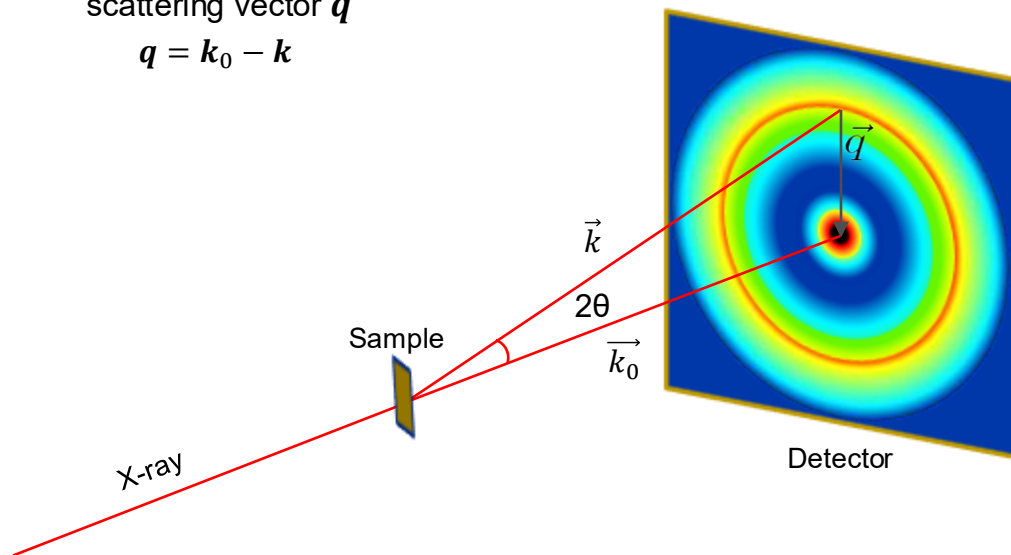


Willmott, P., John Wiley & Sons, Ltd: 2019 (2nd Edition).

$$m\lambda = 2d \sin \theta.$$

Scattering/Diffraction

scattering vector \mathbf{q}
 $\mathbf{q} = \mathbf{k}_0 - \mathbf{k}$



$$|\vec{q}| = q = \frac{4\pi\sin(\theta)}{\lambda}$$

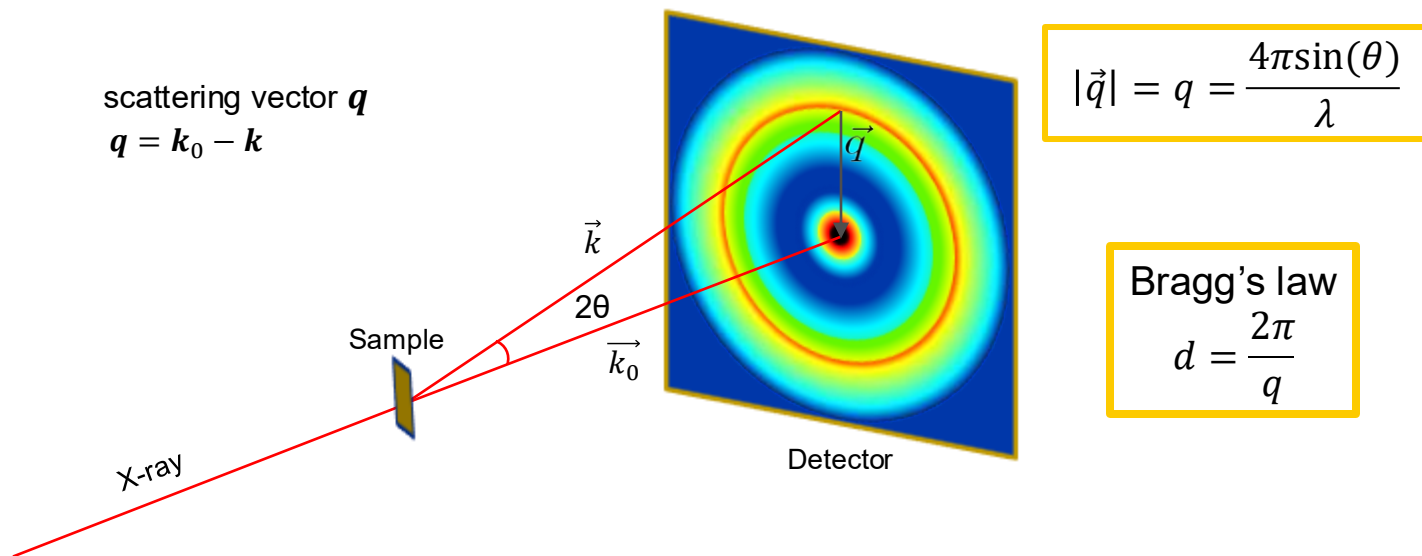
- light $\lambda = 400$ to 600 nm
- X-ray tube $\lambda = 1$ to 2 Å
- Cu $K\alpha = 1.5406$ Å
- synchrotron $\lambda = 0.1$ to 5 Å
- thermal neutrons $\lambda = 1$ to 10 Å
- electrons $\lambda = 0.025$ Å

X-ray energy mostly given in keV
 Electronvolt = eV
 Energy of an electron after being accelerated from rest in a potential of 1 V
 $1 \text{ eV} = 1.6022 \times 10^{-19} \text{ J}$

$E = hc / \lambda$
 h is Planck's constant ($6.6261 \times 10^{-34} \text{ Js}$)
 c is the speed of light ($2.9979 \times 10^8 \text{ m/s}$).

$$\lambda [\text{Å}] = 12.3984/E [\text{keV}]$$

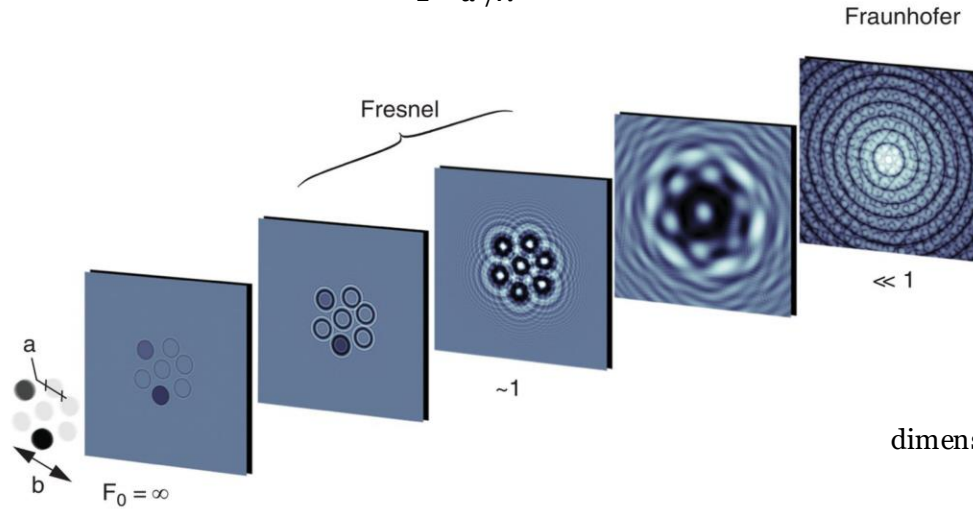
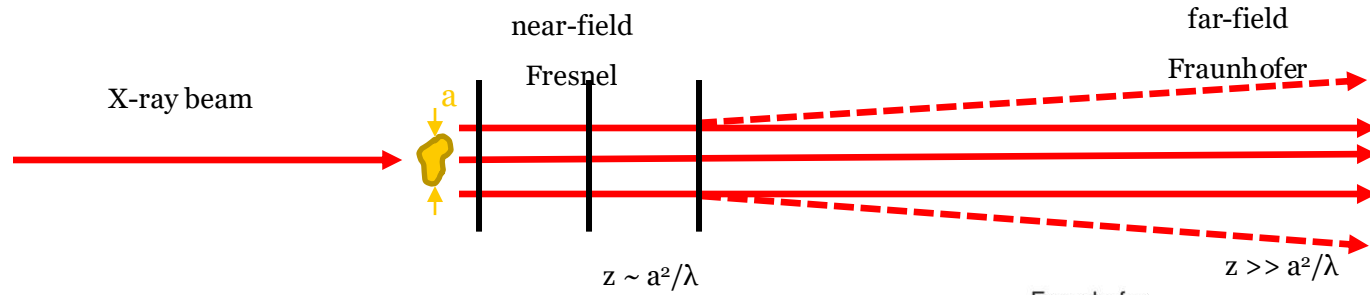
Scattering/Diffraction



SAXS: scattering from variation in electron density distribution, NOT from single atoms as in XRD

larger structures \rightarrow smaller angles
XRD/WAXS: 10 cm detector distance
SAXS: several m detector distance

Far-field Fraunhofer Regim



dimensionless Fresnel number $F_0 = a^2/z\lambda$

Demonstration: Fourier-Transform

Initial Python coding and refactoring:

Brian R. Pauw

<http://www.lookingatnothing.com>

With input from:

Samuel Tardif

Windows compatibility resolution:

David Mannicke

Chris Garvey

Windows compiled version:

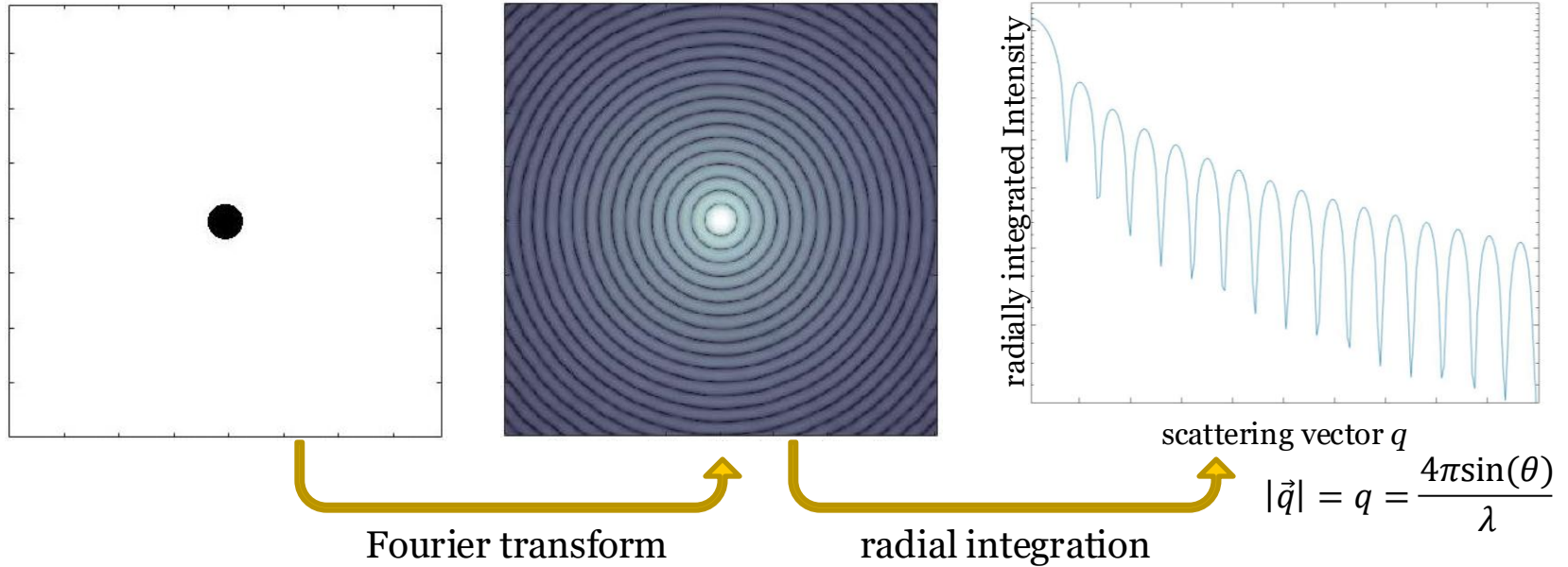
Joachim Kohlbrecher

simulation

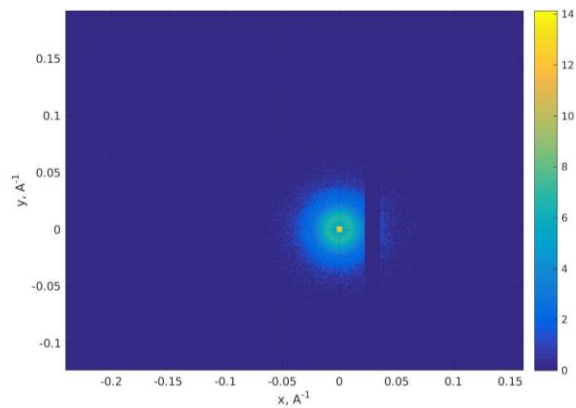
https://phet.colorado.edu/sims/html/wave-interference/latest/wave-interference_en.html

Sample images:

small-angle scattering



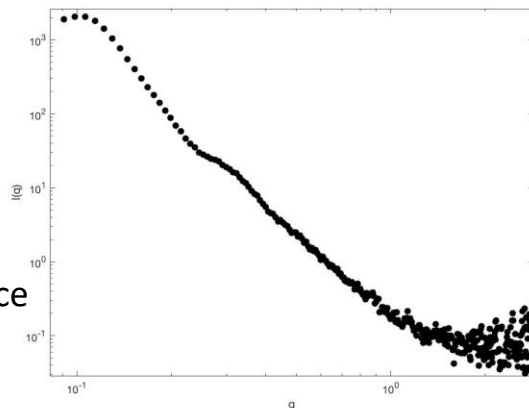
small-angle scattering: first analysis step



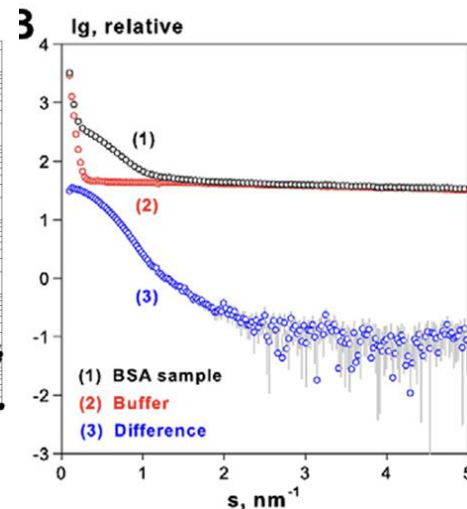
raw data: 2D scattering pattern
(example measured on a Labsource)



beam center
detector distance
wavelength λ
mask

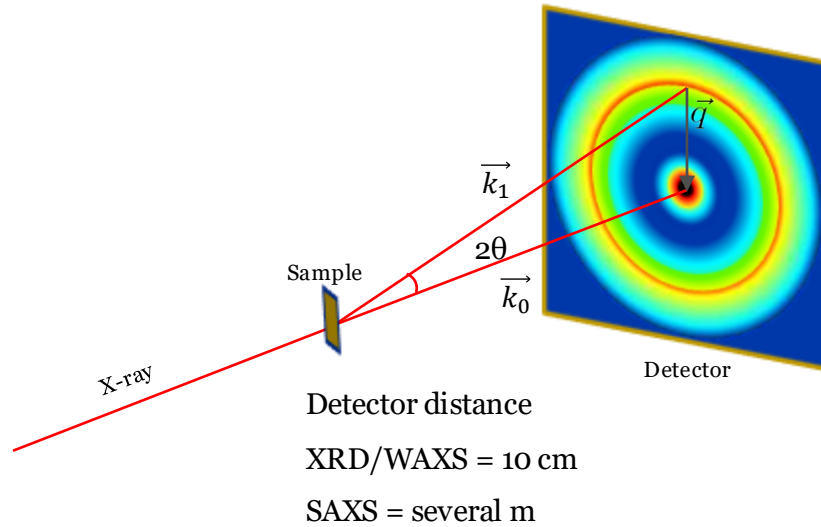


average scattering profile $I(q)$



background subtraction
particles in solution: measure only solvent
solid sample on support: measure only support material

SAXS/WAXS at a labsource

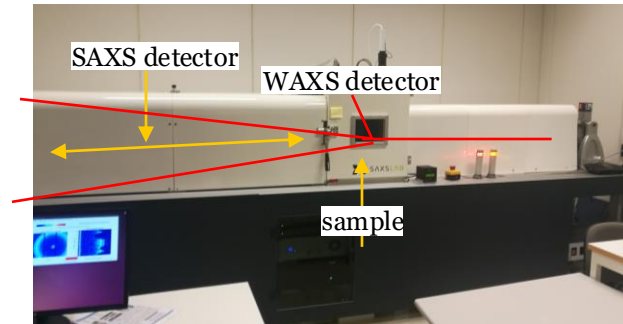


scattering vector q

$$\mathbf{q} = \mathbf{k}_0 - \mathbf{k}$$

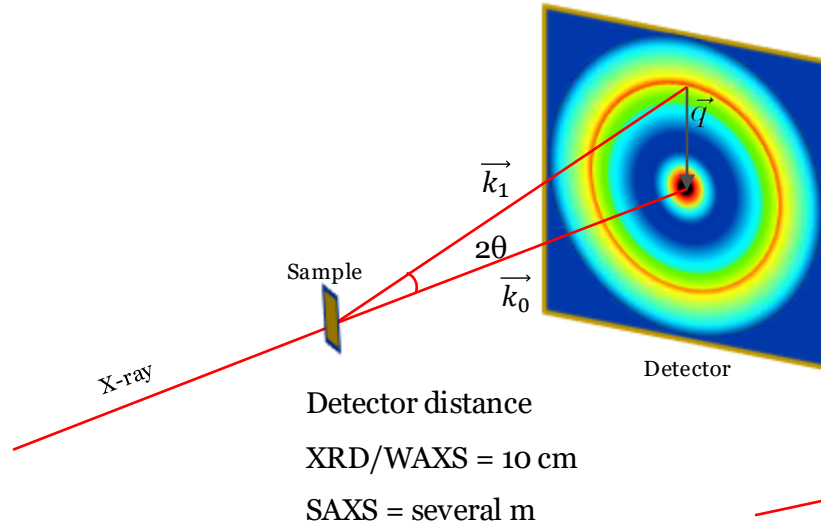
$$|\vec{q}| = q = \frac{4\pi\sin(\theta)}{\lambda}$$

SAXSLAB instrument at CMAL, Chalmers



→ new Labsource SAXS available at EPFL!

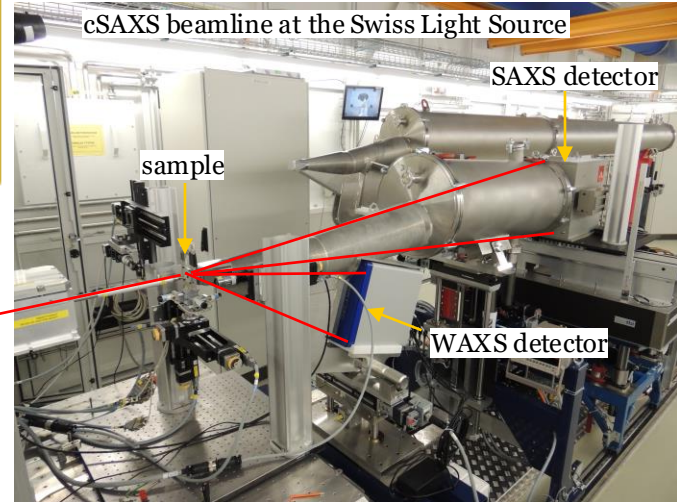
SAXS/WAXS at a synchrotron beamline



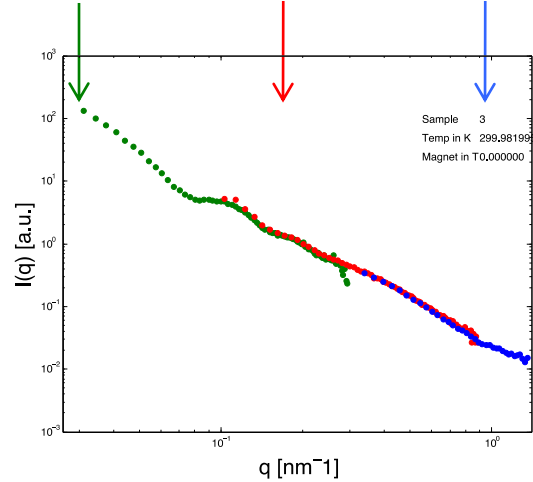
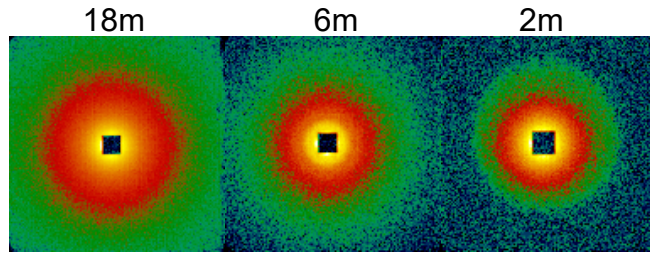
scattering vector q

$$\vec{q} = \vec{k}_0 - \vec{k}_1$$

$$|\vec{q}| = q = \frac{4\pi\sin(\theta)}{\lambda}$$



SANS: radial integration

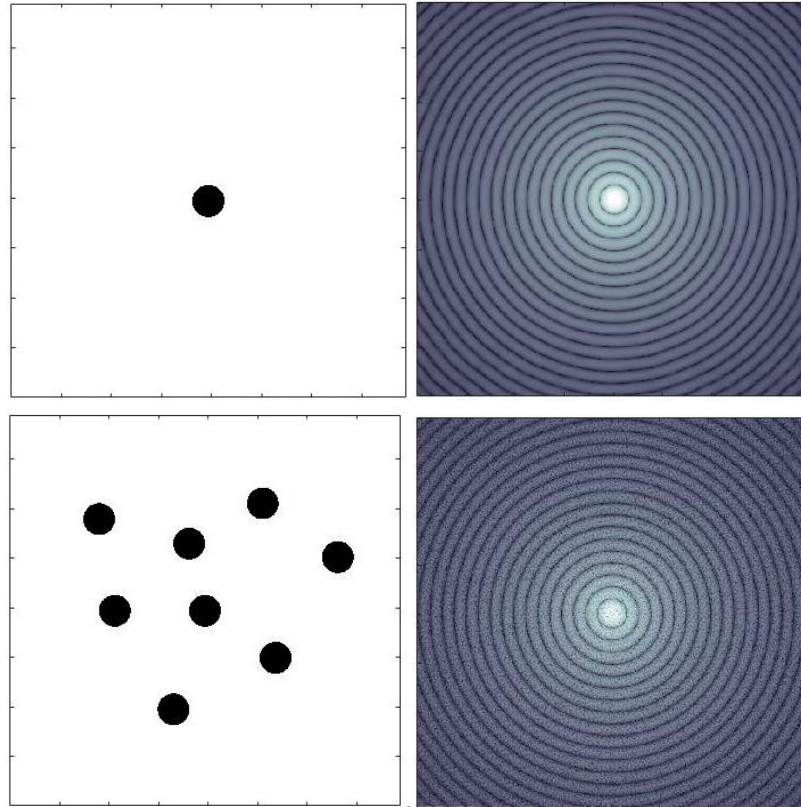


vesicles July 2010



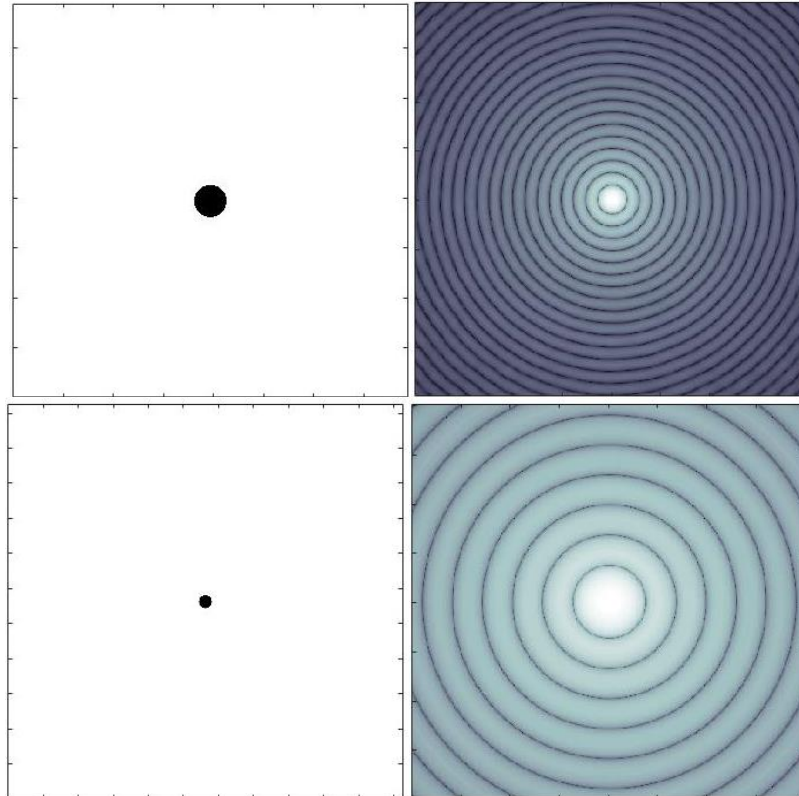
SANS instruments at SINQ

small-angle X-ray scattering



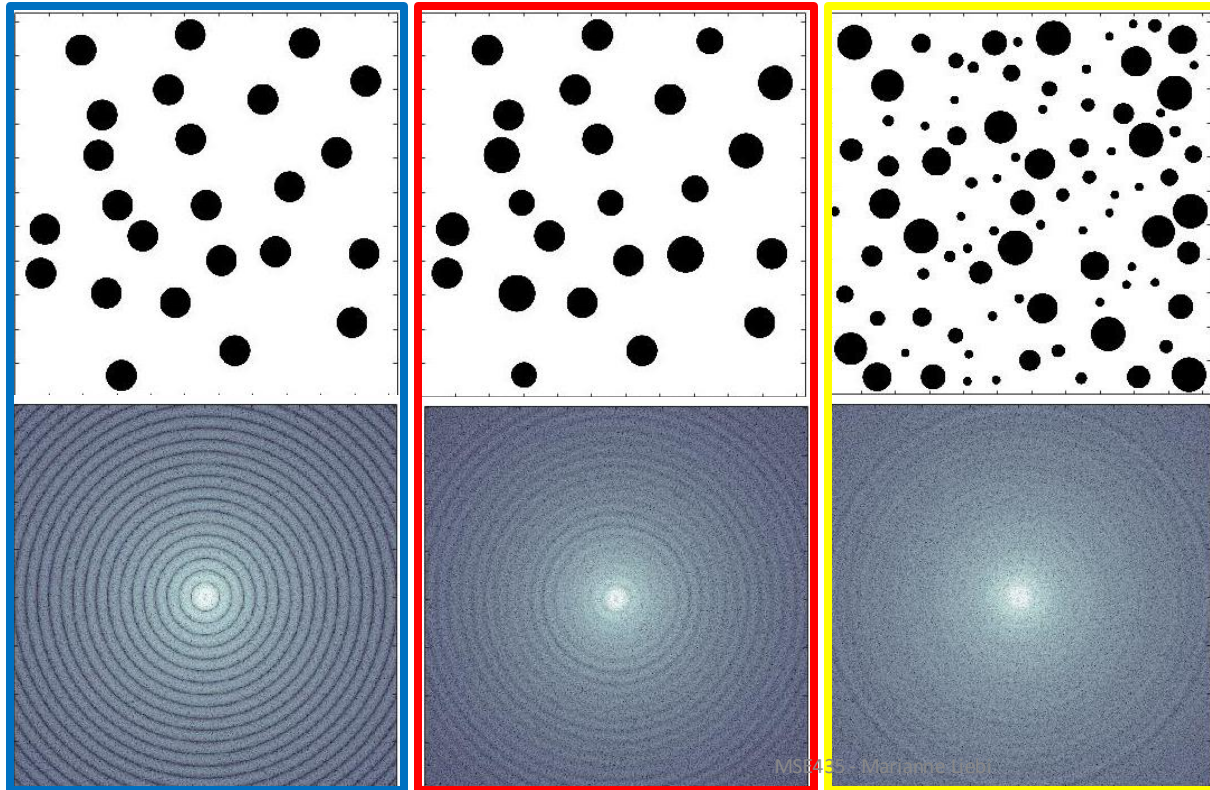
scattering pattern shows
average over particle ensemble

small-angle X-ray scattering size

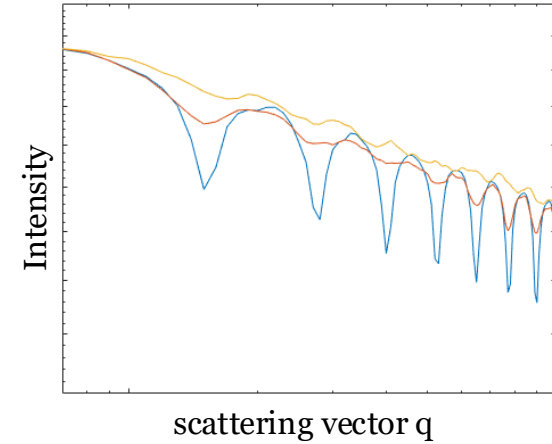


smaller structures scatter
at larger angles

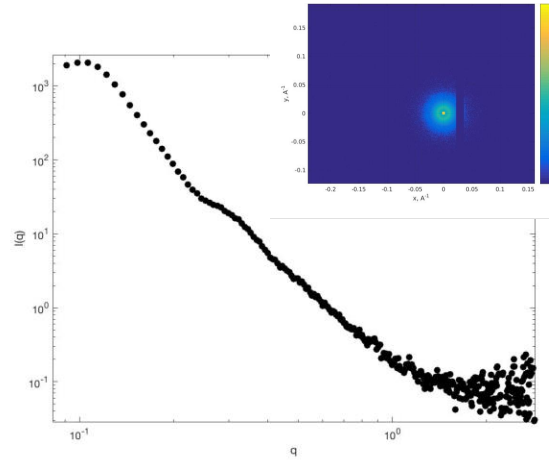
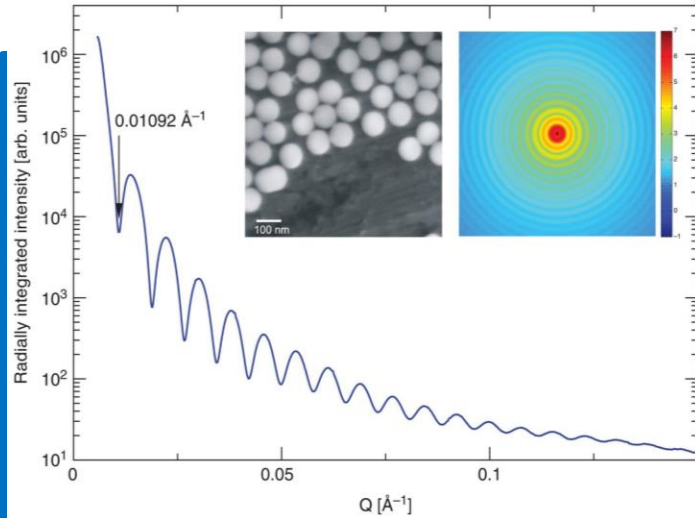
small-angle X-ray scattering polydispersity



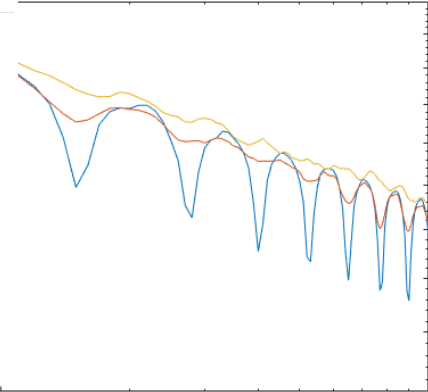
effect of polydispersity



small-angle X-ray scattering polydispersity

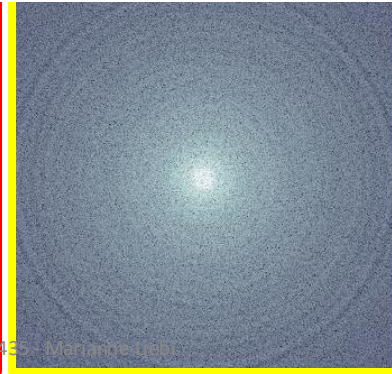
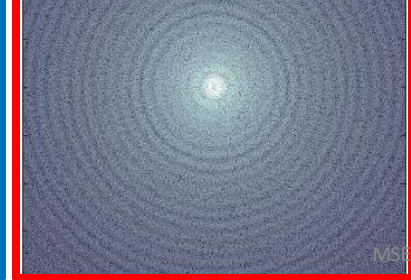


polydispersity

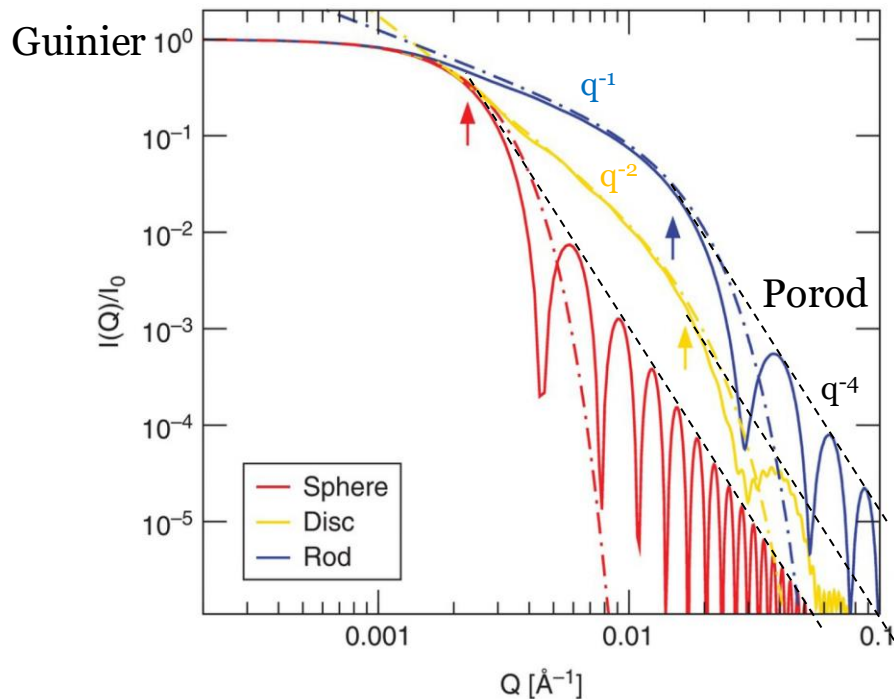


scattering vector q

An Introduction to Synchrotron Radiation: Techniques and Applications, Second Edition. Philip Willmott.
 © 2019 John Wiley & Sons Ltd. Published 2019 by John Wiley & Sons Ltd.



small-angle X-ray scattering size & shape



sphere, disc and rod with the same characteristic length (radius of gyration) \rightarrow same scattering at low q (Guinier regime)

intermediate region depends on fractal dimension

q^{-1} : rod

q^{-2} : disk

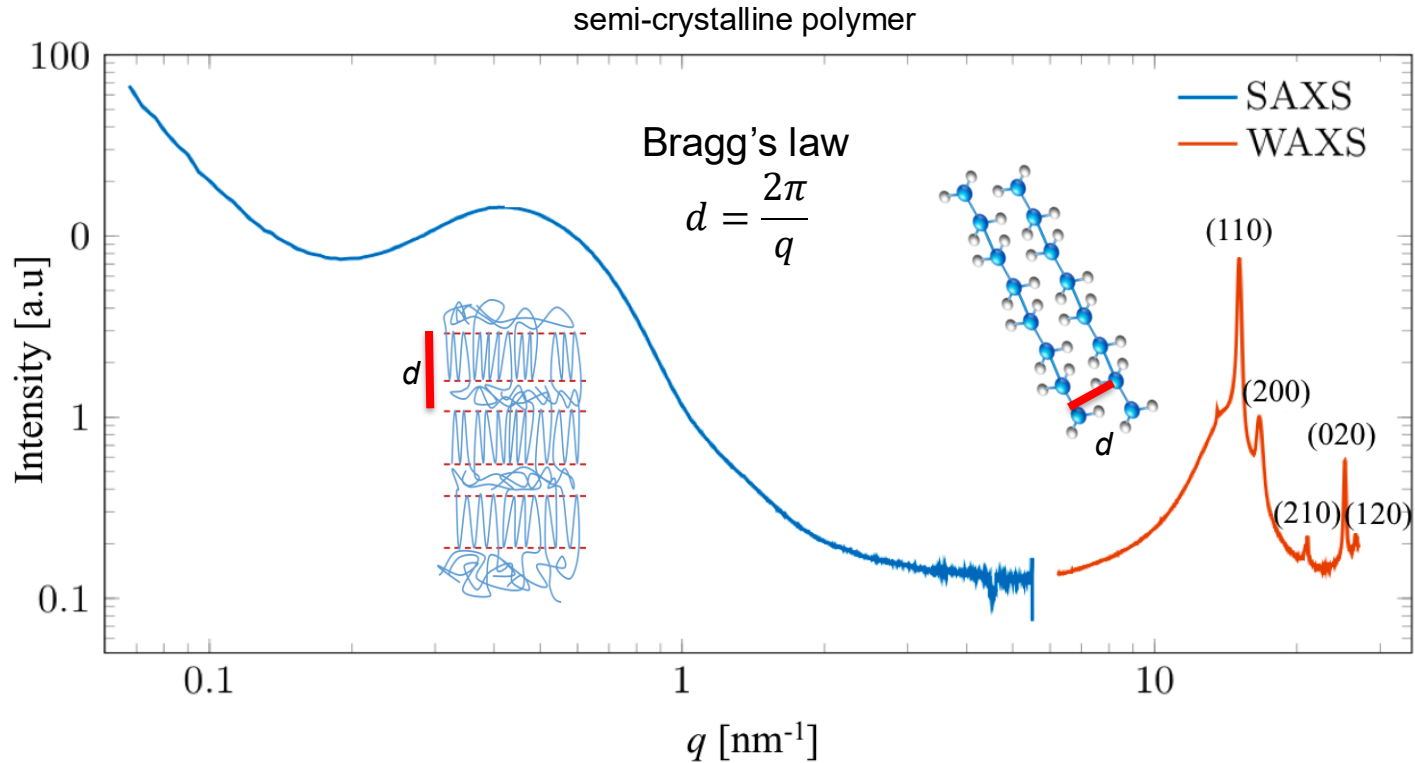
at high q : Porod regime q^{-4}

Small-angle scattering

- Fraunhofer approx. Fourier theorem:
the field distribution at a distant detector is the Fourier transform of the electric field distribution in the exit plane of a sample
BUT we don't measure field but the intensity, which is the squared field: complex quantity:
complex part (the phase) get lost → **the phase problem**

- we cannot directly calculate back the particles shape and size, different approaches to retrieve information from the scattering pattern
 - **model independent**
 - mathematically model the SAXS curve
 - pair distance distribution function (PDDF)
 - iterative phase retrieval

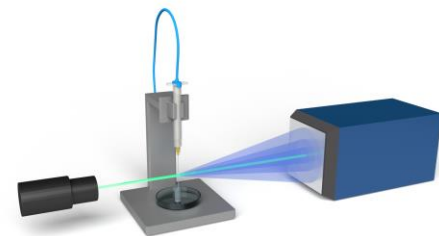
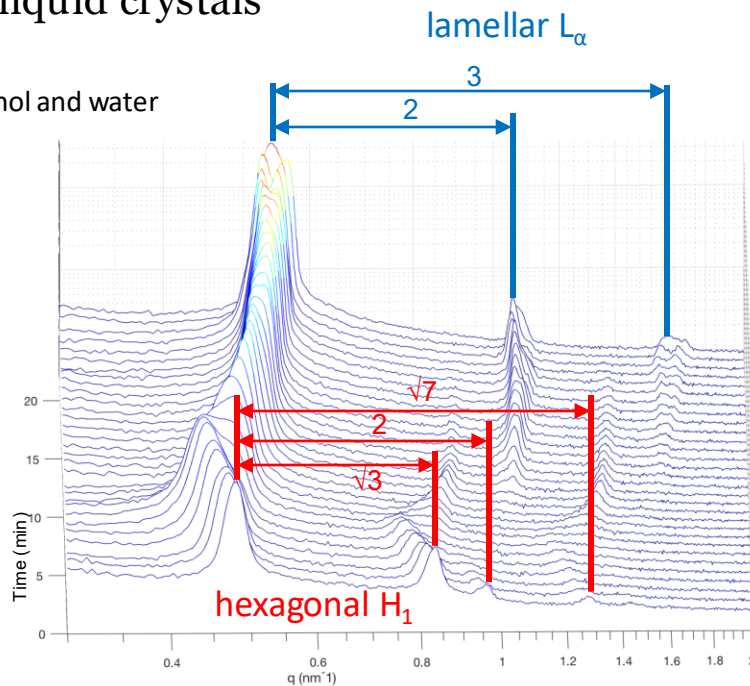
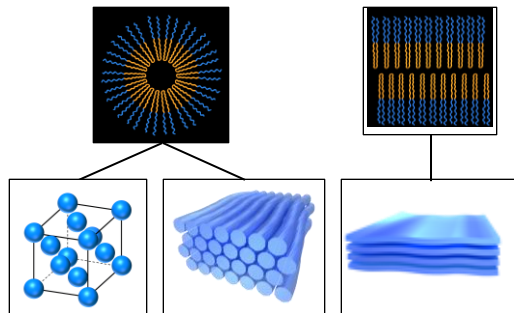
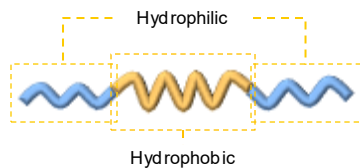
Small-angle scattering: any peaks?



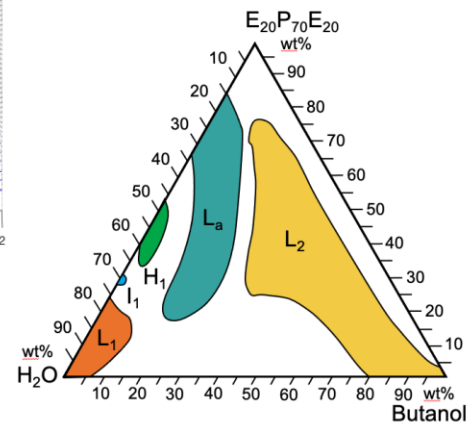
Small-angle scattering: any peaks?

3D printing of lyotropic liquid crystals

Pluronic F-127 (EO₁₀₀PO₇₀EO₁₀₀), 1-butanol and water



time-resolved measurements of phase changes after 3D printing



Small-angle scattering

low q : information about interactions between the particles and particle size, no information about shape of particle

intermediate q : in the order of the particle size, particle shape

high q : Porod's region contrast at the interface between the particle and their surrounding, measure of surface area

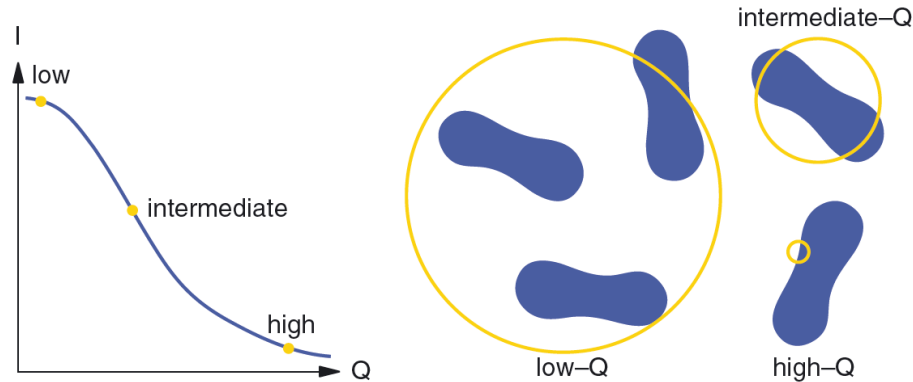
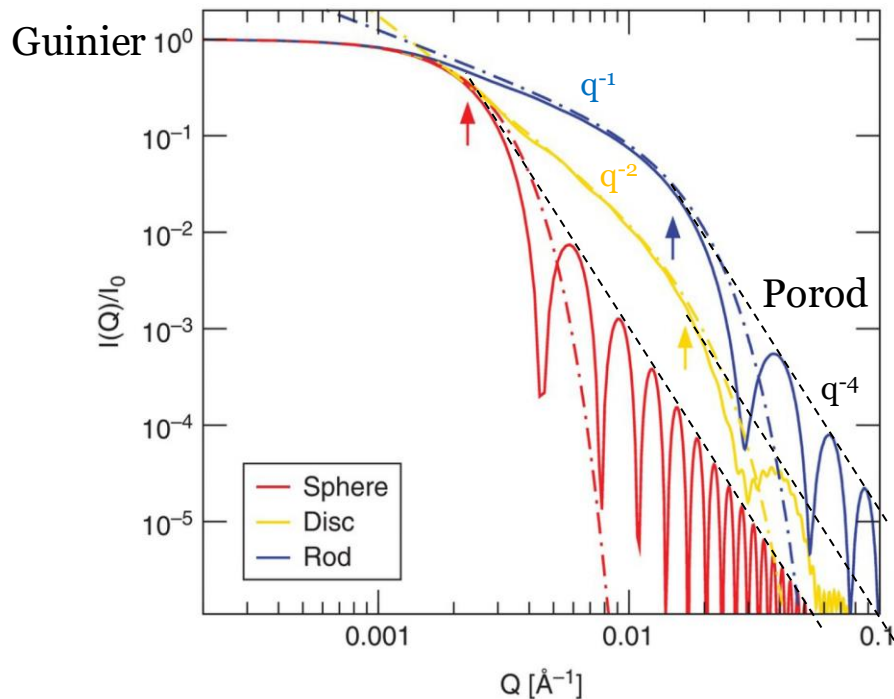


Figure 5.67 *The three Q -domains of SAXS.*

small-angle X-ray scattering size & shape



sphere, disc and rod with the same characteristic length (radius of gyration) \rightarrow same scattering at low q (Guinier regime)

intermediate region depends on fractal dimension

q^{-1} : rod

q^{-2} : disk

at high q : Porod regime q^{-4}

Guinier approximation

- Radius of gyration R_G : “weight average” of all radii present in the sample in analogy to mechanics



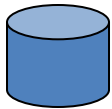
solid sphere radius R : $R_G^2 = \frac{3}{5} R^2$



thin rod length L : $R_G^2 = \frac{1}{12} L^2$



thin disc radius R : $R_G^2 = \frac{1}{2} R^2$

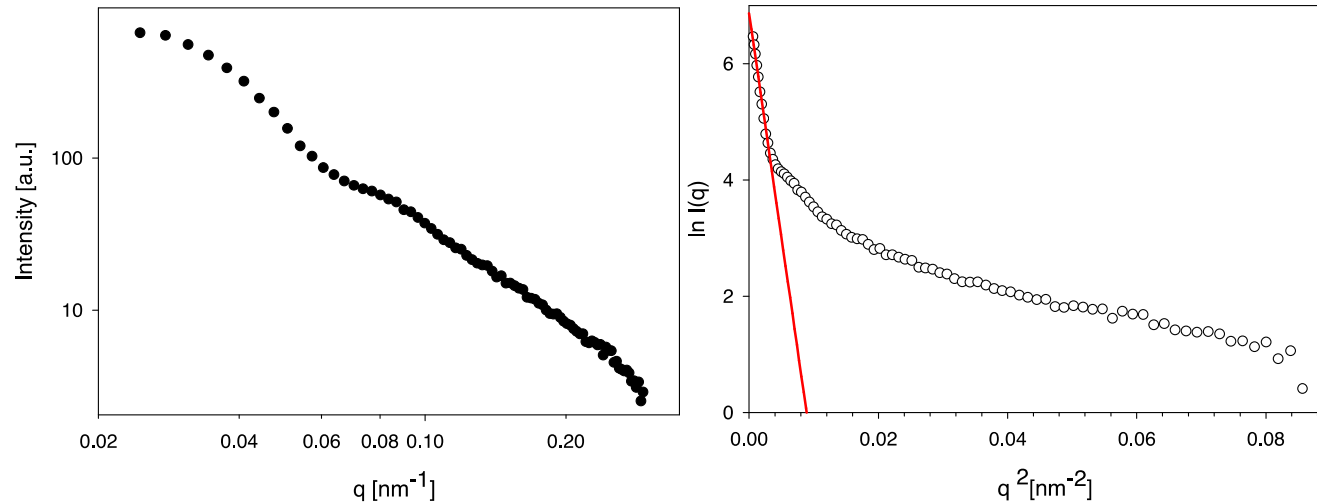


cylinder of height h and radius R : $R_G^2 = \frac{R^2}{2} + \frac{h^2}{12}$

Guinier approximation

Guinier approximation valid only in the region of small q values, R_G can be derived

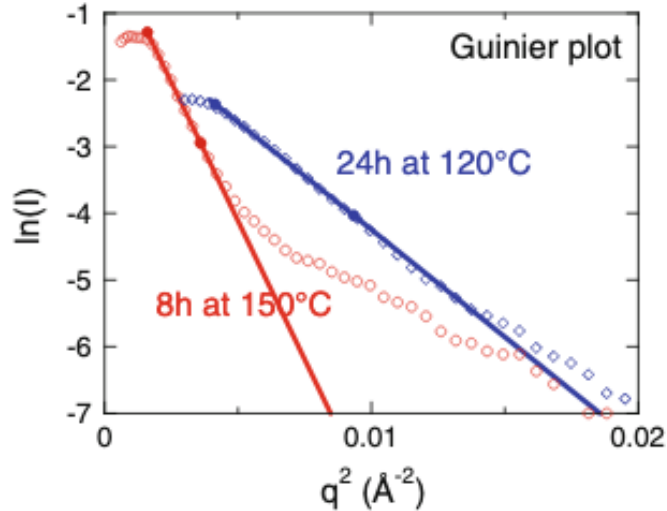
$$I(q) \approx I(0)e^{-(1/3)q^2 R_G^2}$$



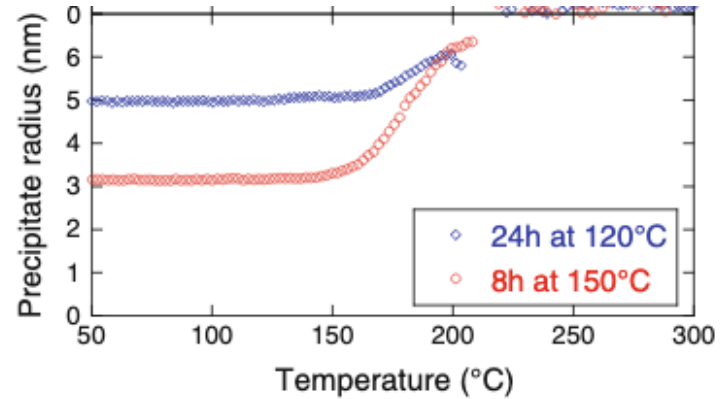
A not existing linear range indicates the presence of very large structures which scatter at low q , perhaps outside the accessible q range \rightarrow change detector distance, change λ , check with SLS

SAXS on metal alloys

SAXS measurements on Al-Mg-Li alloy for two aging conditions



Evolution of precipitate radius during ramp heating experiments on these two initial aging conditions



Deschamps A. and De Geuser F. Metallurgical and Materials Transactions A, 44, 2013, 77-86

Small-angle scattering: Power law

Slope of the scattering curve: power law behavior

q^{-D} with D the **fractal dimension**

How does the mass changes as a function of the size

rod-like D=1

disk-like D=2

in general: the higher D, the more compact is the structure

D=4 Porod scattering

→ sharp interphase of two phases, information about surface area

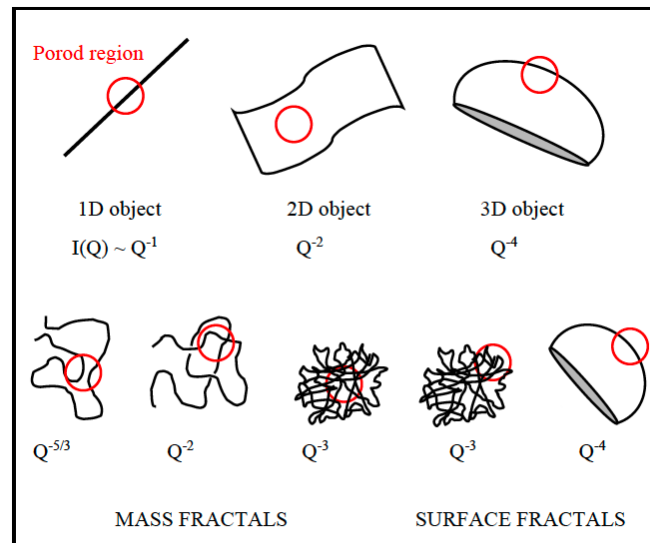
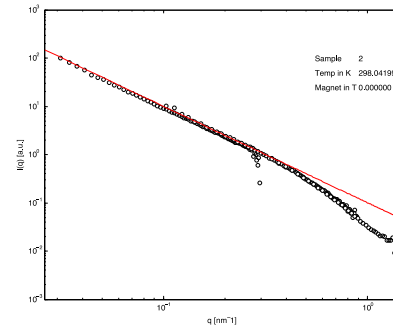
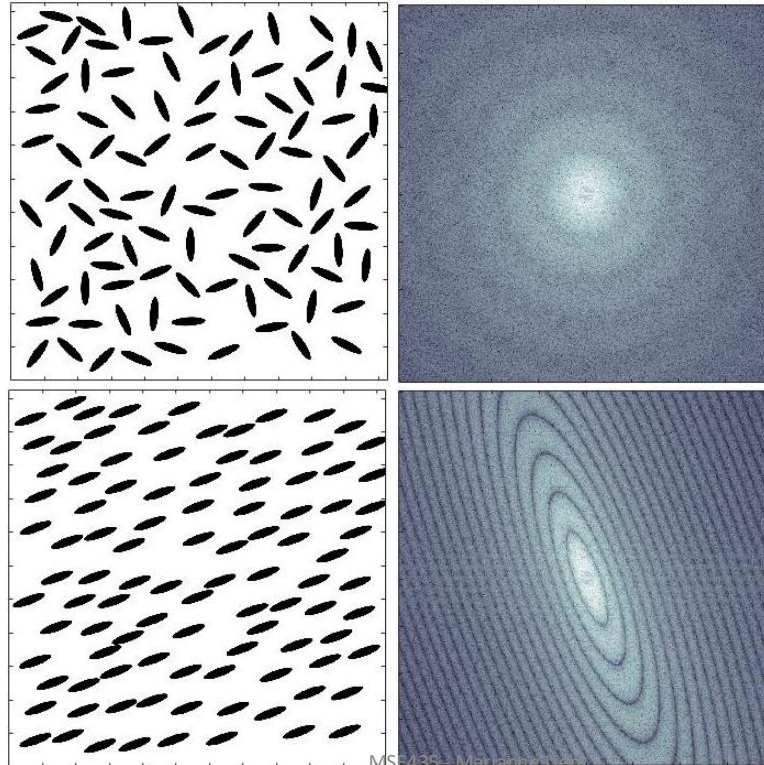


Figure 7: Assortment of Porod law behaviors for different shape objects.

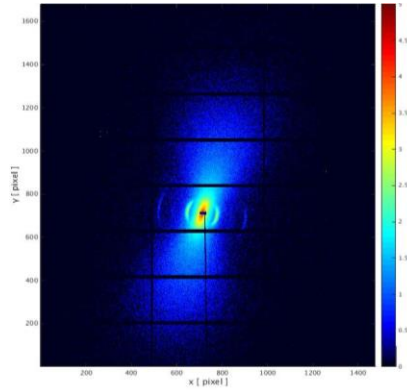
small-angle X-ray scattering: anisotropic particles



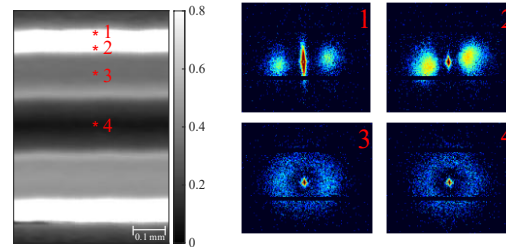
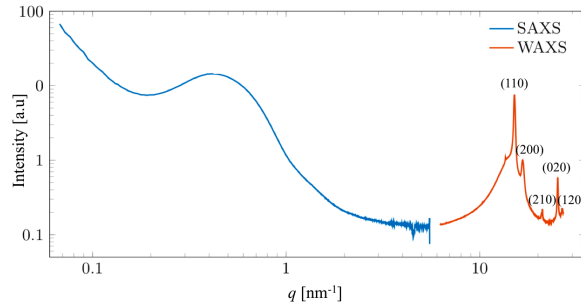
anisotropic and aligned
particles produce anisotropic
scattering

→ direct determination of
orientation of nanoparticles!

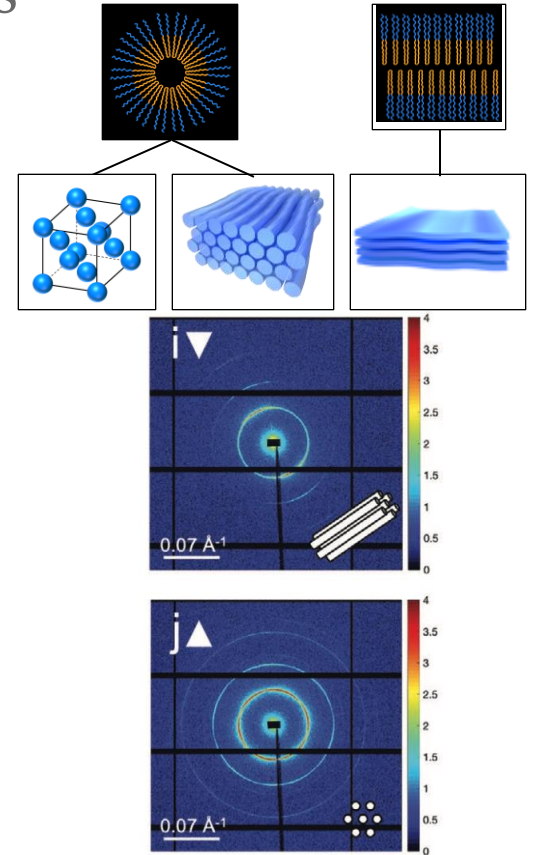
SAXS of anisotropic materials



SAXS signal from mineralized collagen in human bone

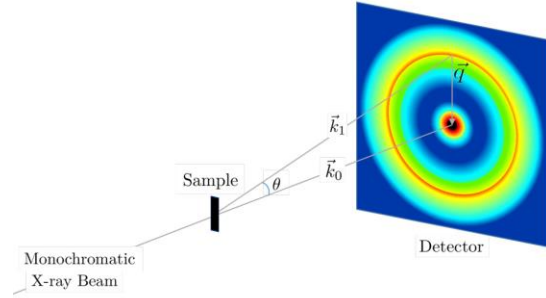
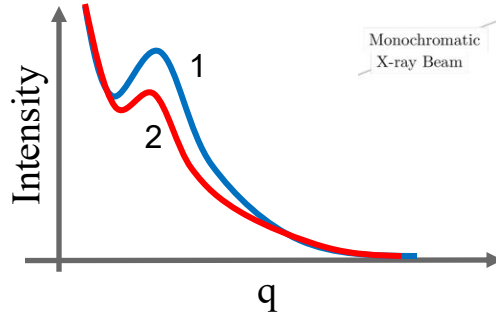
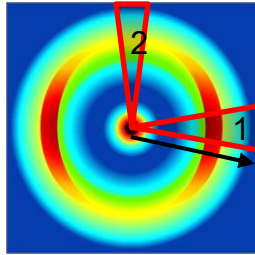


SAXS signal from different layers in injection-molded polymers



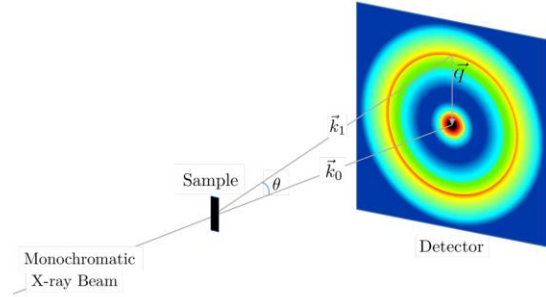
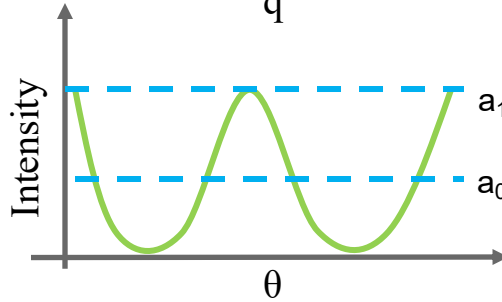
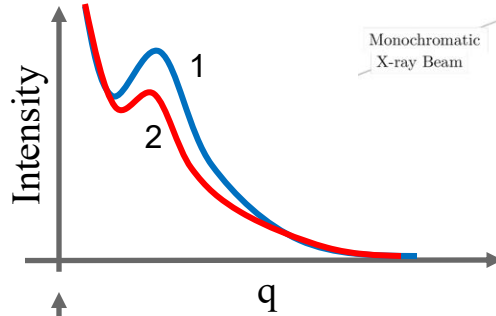
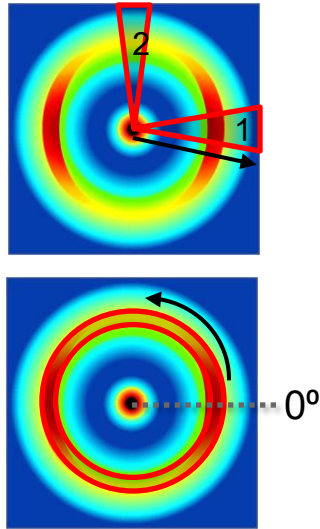
SAXS signal from liquid crystals oriented in flow

SAXS of anisotropic materials



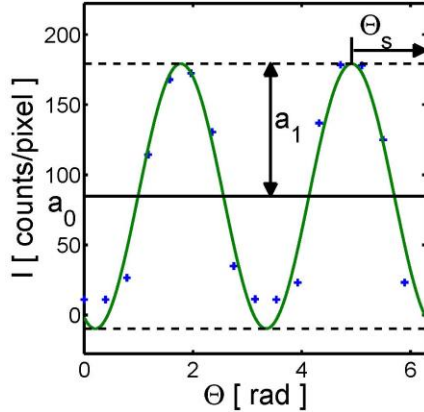
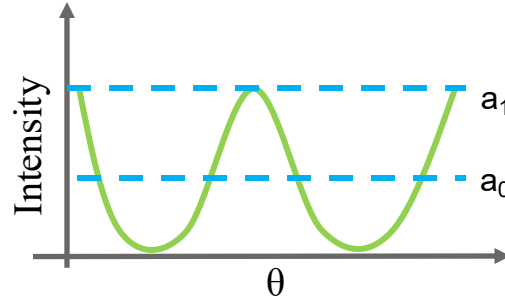
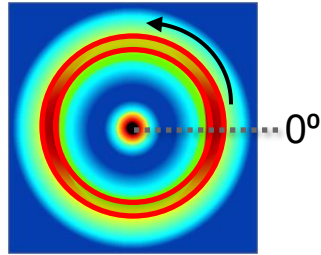
$$|\vec{q}| = q = \frac{4\pi}{\lambda} \sin \frac{\theta}{2}$$

SAXS of anisotropic materials



$$|\vec{q}| = q = \frac{4\pi}{\lambda} \sin \frac{\theta}{2}$$

SAXS of anisotropic materials



$$I(n_{\Theta}) \approx a_0 + a_1 \cos(2\pi n_{\Theta}/N_{\Theta} - \Theta_s)$$

$\frac{a_0}{a_1}$ degree of orientation

Bunk, O. *et al.* Multimodal x-ray scatter imaging. *New Journal of Physics* **11**, (2009).

Small-angle scattering

- Fraunhofer approx. Fourier theorem:
the field distribution at a distant detector is the Fourier transform of the electric field distribution in the exit plane of a sample
BUT we don't measure field but the intensity, which is the squared field: complex quantity:
complex part (the phase) get lost → **the phase problem**

- we cannot directly calculate back the particles shape and size, different approaches to retrieve information from the scattering pattern
 - model independent
 - **mathematically model the SAXS curve**
 - pair distance distribution function (PDDF)
 - iterative phase retrieval

Mathematical modelling of Small-angle scattering

$$I(q) = (\rho_P - \rho_M)^2 N_P V_P^2 P(q) S(q)$$

$\rho_P - \rho_M$: contrast in scattering length density between particle and matrix

N_P : number of particles

V_P : volume of particles

Formfactor $P(q)$

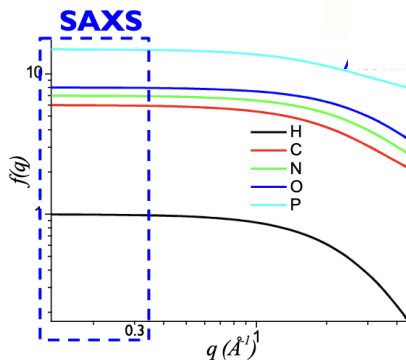
Intra-particle interference
shape, size

Structure factor $S(q)$

Inter-particle interference
spacing, interactions

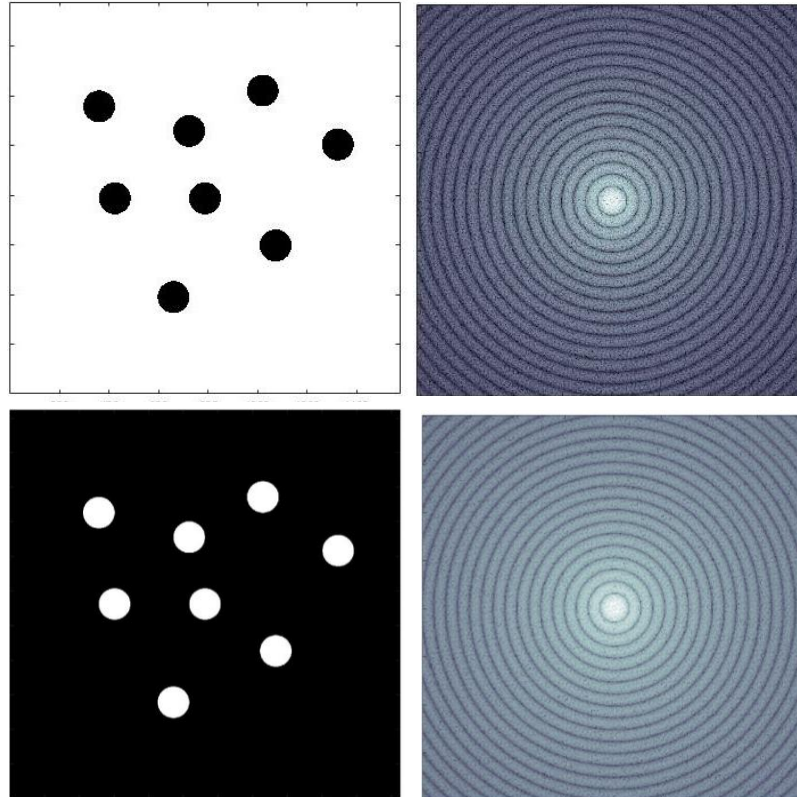
for X-rays: electron density difference

for neutrons: neutron scattering length density difference



note that the atomic form factor in the SAXS regime is a constant

small-angle X-ray scattering



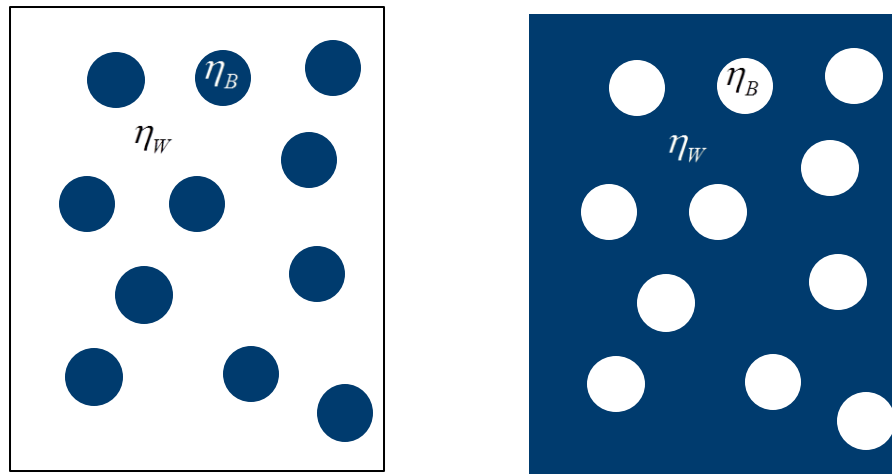
Babinet's principle:

particle vs. pores

same diffraction pattern apart
from overall intensity

Babinet's principle: particles or pores?

two structures where only the scattering length densities are exchanged give the same scattering (incoherent scattering may be different)

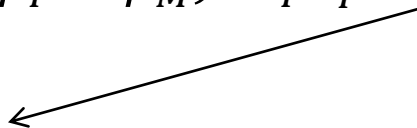


$$I(\mathbf{q}) \propto (\eta_B - \eta_W)^2$$

- contrast is relative
- loss of phase information (is $\eta_B > \eta_W$?)

Model dependent fitting: Formfactor

$$I(q) = (\rho_P - \rho_M)^2 N_P V_P^2 P(q) S(q)$$



3.1.1. Sphere.

3.1. Spheres & Shells

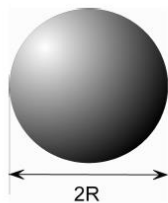


FIGURE 3.1. Sphere with diameter $2R$

$$I_{\text{sphere}}(Q, R) = K^2(Q, R, \Delta\eta) \quad (3.1a)$$

with

$$K(Q, R, \Delta\eta) = \frac{4}{3}\pi R^3 \Delta\eta^3 \frac{\sin QR - QR \cos QR}{(QR)^3} \quad (3.1b)$$

The forward scattering for $Q = 0$ is given by

$$\lim_{Q \rightarrow 0} I_{\text{sphere}}(Q, R) = \left(\frac{4}{3}\pi R^3 \Delta\eta \right)^2$$

Input Parameters for model Sphere:

R: radius of sphere R

--: not used

---: not used

eta: scattering length density difference between particle and matrix $\Delta\eta$

form factor of a sphere

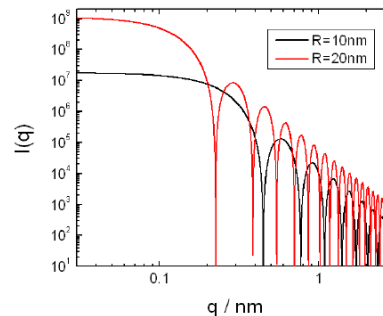
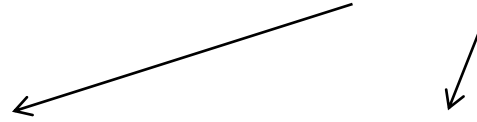


FIGURE 3.2. Scattering intensity of spheres with radii $R = 10\text{nm}$ and $R = 20\text{nm}$. The scattering length density contrast is set to 1.

Model dependent fitting: Structure factor

$$I(q) = (\rho_P - \rho_M)^2 N_P V_P^2 P(q) S(q)$$

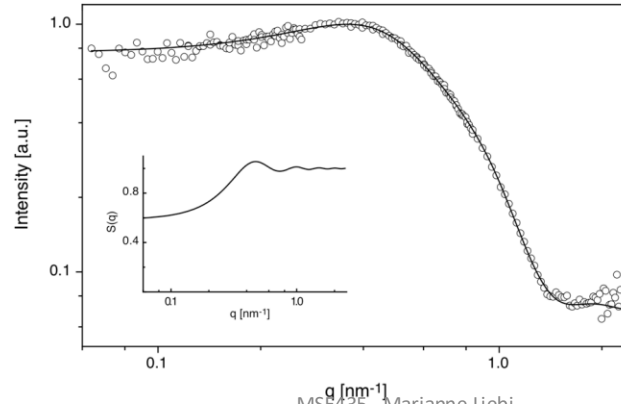


Formfactor $P(q)$

Structure factor $S(q)$

Interacting particles

→ Measure different concentrations



example: Phospholipid micelle
ellipsoidal form factor

hard sphere structure factor (hard
sphere radius larger than radius of
micelles)

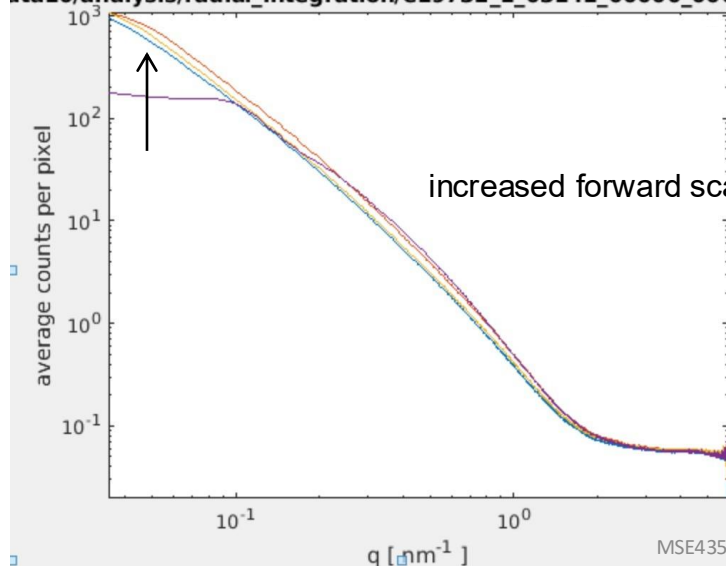
→ self-assembly & surfactants

Model dependent fitting: Structure factor

$$I(q) = (\rho_P - \rho_M)^2 N_P V_P^2 P(q) S(q)$$



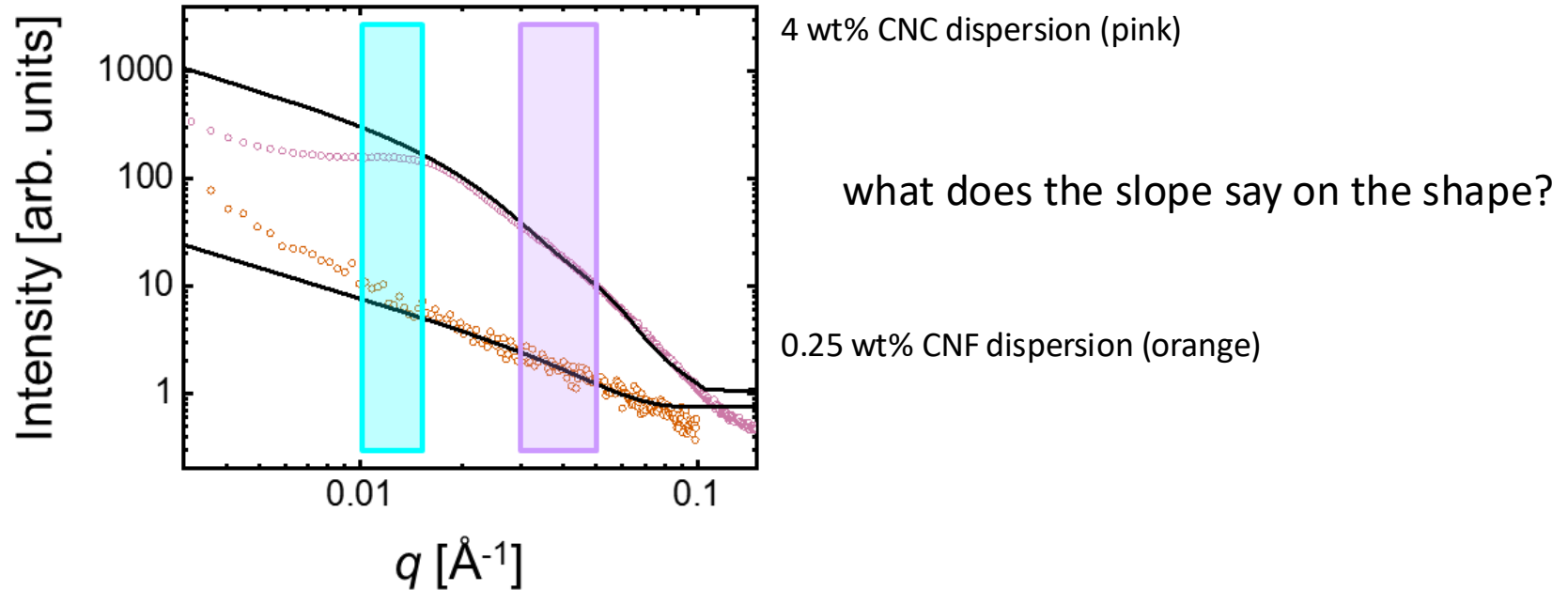
ata10/analysis/radial_integration/e19732_1_03141_00000_00000



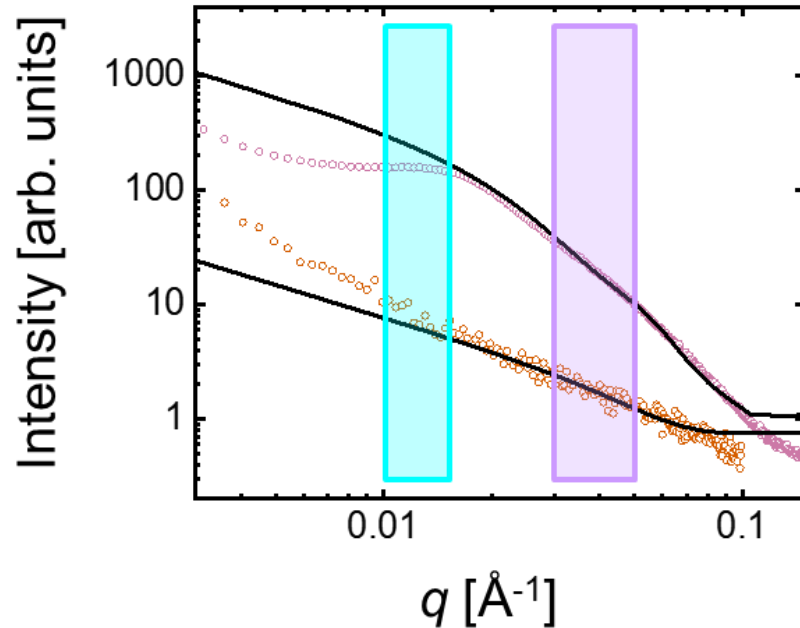
Structure factor $S(q)$

Interacting particles

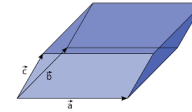
Example: cellulose nano crystals (CNC) and cellulose nano fibrils (CNF)



Example: cellulose nano crystals (CNC) and cellulose nano fibrils (CNF)



4 wt% CNC dispersion (pink): parallelepiped shape with cross section dimensions of 6 nm and 18 nm as form factor (black)

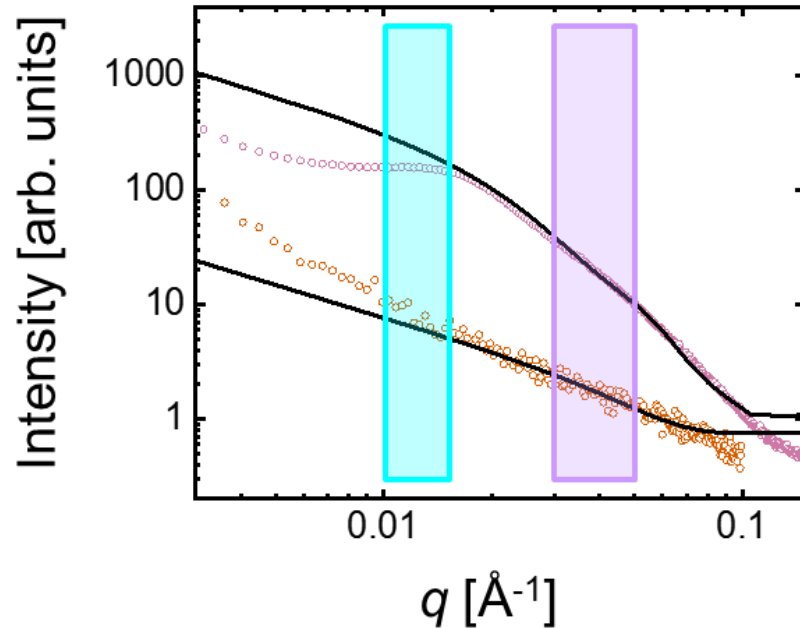


0.25 wt% CNF dispersion (orange): cylindrical shape with particle radius of 6 nm, length longer than the measured q -range as form factor (black)

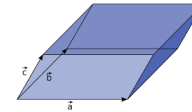


what indicates the deviation from fit with a structure factor at low q ?

Example: cellulose nano crystals (CNC) and cellulose nano fibrils (CNF)



4 wt% CNC dispersion (pink): parallelepiped shape with cross section dimensions of 6 nm and 18 nm as form factor (black) at low q (blue box) deviation due to a **structure factor contribution for repulsive interaction**



0.25 wt% CNF dispersion (orange): cylindrical shape with particle radius of 6 nm, length longer than the measured q -range as form factor (black) at low q (starting from blue box) deviation due to a **structure factor contribution for attractive interaction**

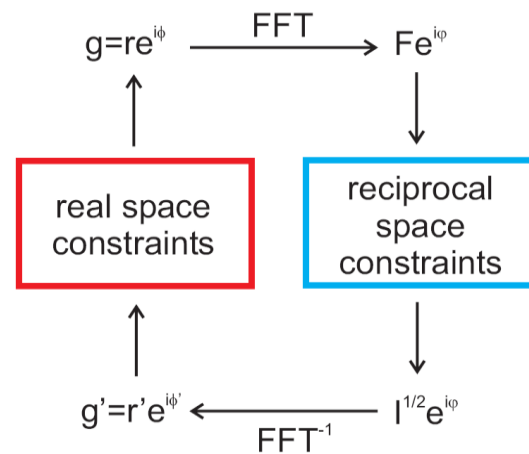
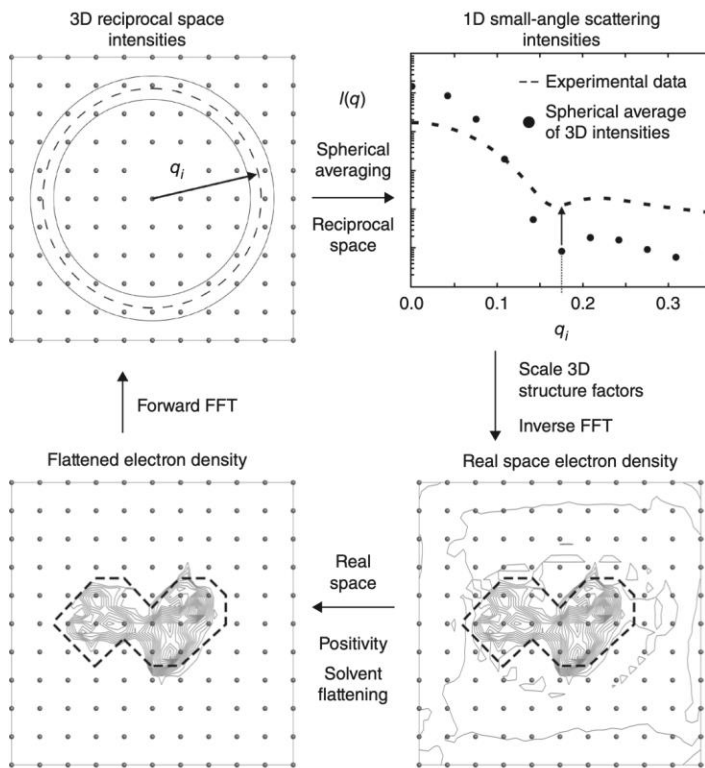


Small-angle scattering

- Fraunhofer approx. Fourier theorem:
the field distribution at a distant detector is the Fourier transform of the electric field distribution in the exit plane of a sample
BUT we don't measure field but the intensity, which is the squared field: complex quantity:
complex part (the phase) get lost → **the phase problem**

- we cannot directly calculate back the particles shape and size, different approaches to retrieve information from the scattering pattern
 - model independent
 - mathematically model the SAXS curve
 - pair distance distribution function (PDDF)
 - **iterative phase retrieval**

SAXS analysis: iterative approach



Grant, T. D., *Nature Methods* **2018**, *15*, 191.

SAXS analysis: iterative approach

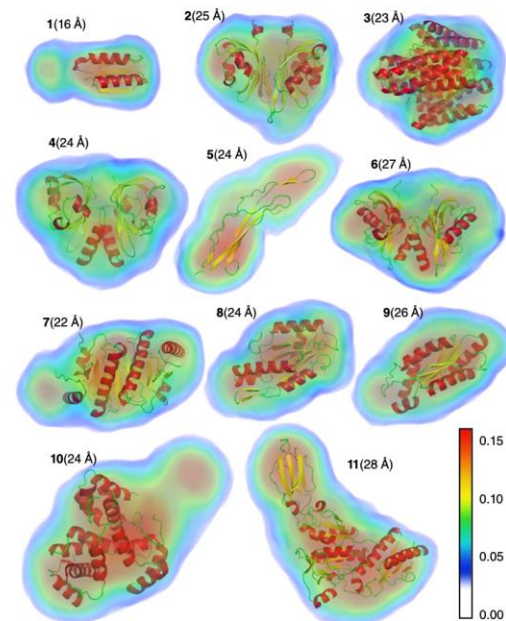
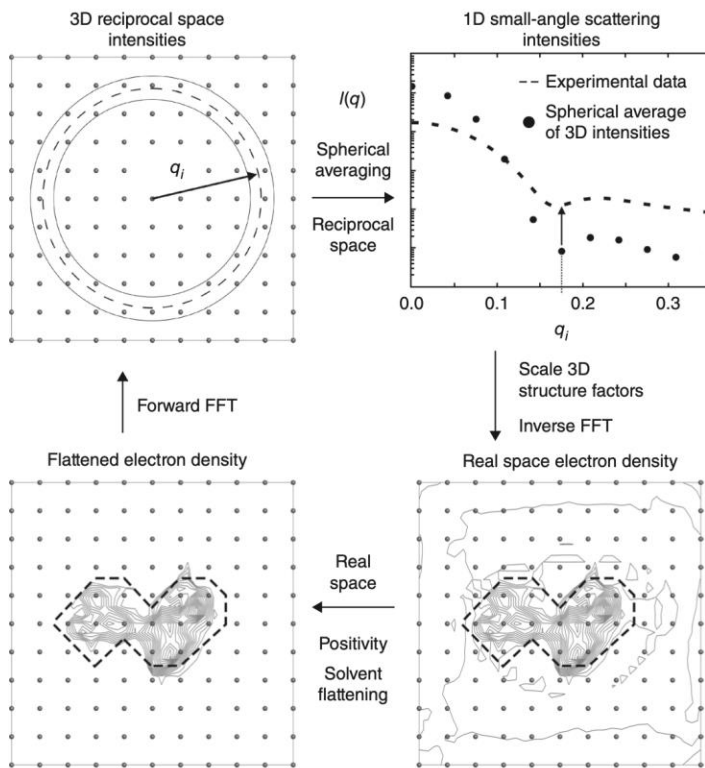
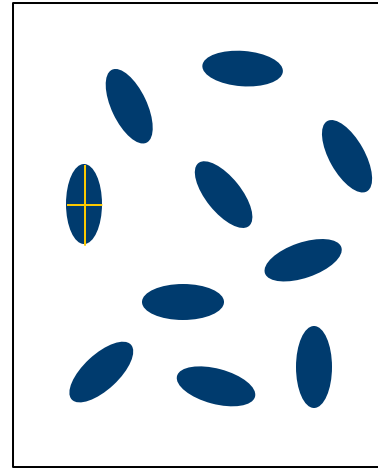
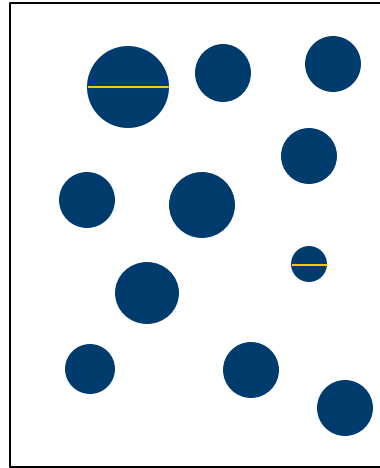


Figure 2 | Electron density reconstructions from experimental solution scattering data for samples 1–11 (**Supplementary Table 1**). Electron densities are shown as volumes colored according to density (color bar indicates electron density values in $e^-/\text{\AA}^3$). X-ray crystal structures (for PDB IDs, see **Supplementary Table 1**) are shown in cartoon format. Estimated resolutions of the solution scattering reconstructions are shown next to sample ID (see Online Methods).

Grant, T. D., *Nature Methods* **2018**, *15*, 191.

Polydispersity is the devil...

Small-angle scattering is a statistical method of all length scales in a sample
particle polydispersity or particle shape?



X-rays vs. neutrons

- Wavelengths in the order of atomic distances
- Penetrate into matter from μm to many cm deep

- scattered by nucleus of atoms
- scattering contrast depends on mass number A , is isotope-specific

$$n_{\text{neutrons}} = \sqrt{\frac{E_{\text{kin}} - \bar{V}}{E_{\text{kin}}}} \cong 1 - \frac{\bar{b} n_a}{2\pi} \lambda^2$$

→ contrast matching!

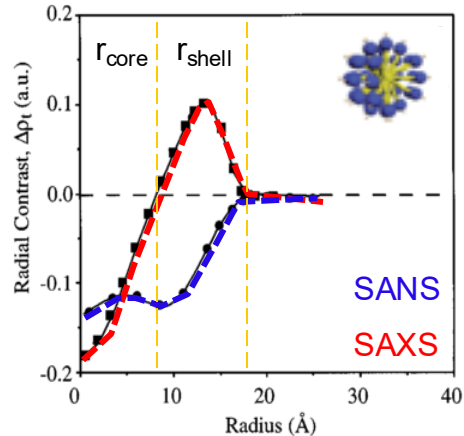
- Interact with magnetic moment in shell of atom
→ magnetic structures and magnetism

- scattered by electronic shell of atoms
- Scattering contrast proportional to order number (number of electrons)

$$n_{\text{x-ray}} = 1 - \frac{\bar{Z} r_e n_a}{2\pi} \lambda^2$$

- Larger flux possible → faster, lower concentrations, smaller beam

SAXS vs. SANS as complementary contrast



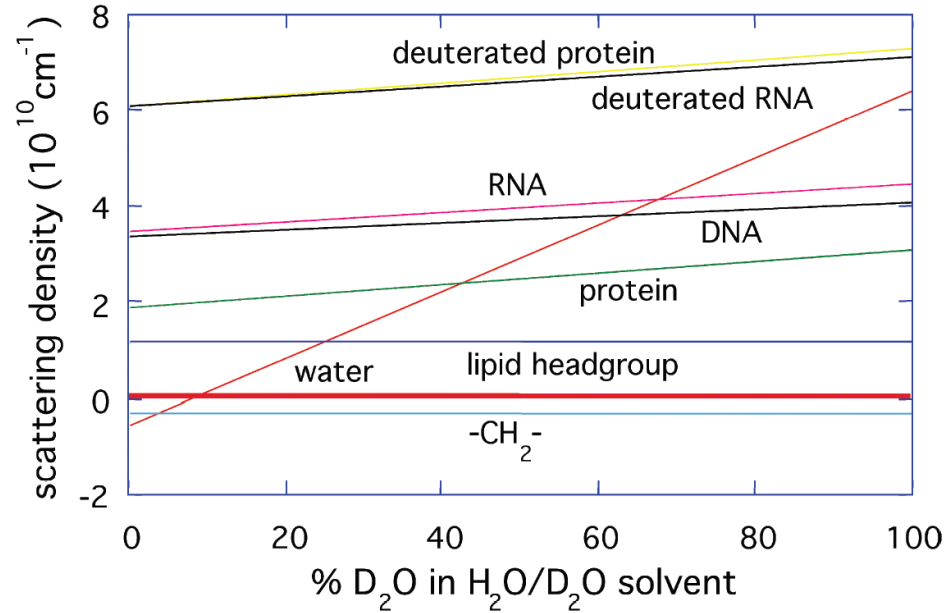
SANS contrast is mainly between the full micelle and the solvent

→ overall size of micelles

SAXS headgroups have a higher contrast than lipid tails

→ internal structures

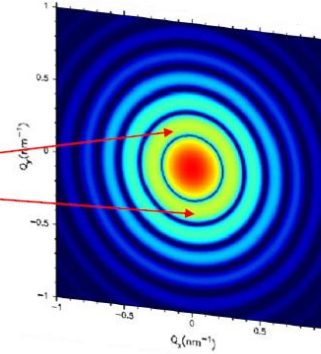
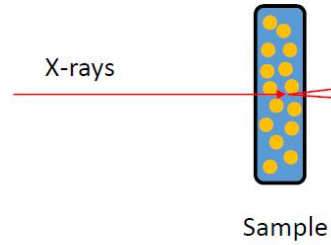
Contrast matching in SANS



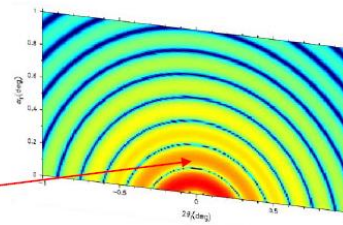
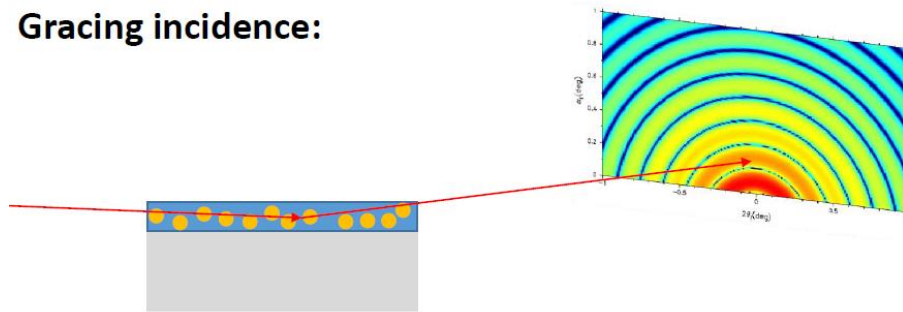
Scattering length density different for isotopes! Hydrogen and Deuterium!

SAXS at gracing incidence: GISAXS

Transmission:



Gracing incidence:



Extensive article on GISAXS including theoretical background, experimental consideration and application examples:

Renaud, G., Lazzari, R., & Leroy, F. (2009). Probing surface and interface morphology with Grazing Incidence Small Angle X-Ray Scattering. *Surface Science Reports*, 64(8), 255–380. <https://doi.org/10.1016/j.surfrep.2009.07.002>

7.	Examples of extensive data analysis of GISAXS patterns	306
7.1.	First example: Pt/MgO(001)	307
7.2.	Second example: Pd/MgO(001)	307
7.3.	Third example: Au/TiO ₂ (110)	308
7.4.	Diffuse scattering due to correlations	308
7.4.1.	Evidence of diffuse scattering in GISAXS	308
7.4.2.	Estimated diffuse scattering in GISAXS	308
7.4.3.	Size-position correlation deduced from GISAXS	309
8.	Non-LHV GISAXS experiments	310
8.1.	Embedded metallic nanoparticles	310
8.1.1.	Granular solids and multilayers of metallic clusters embedded into oxide matrices	310
8.1.2.	Encapsulated Ag, Fe, Pt and Au nanoparticles into carbon and boron nitride	311
8.1.3.	Embedded clusters into glass by ion implantation	315
8.2.	Porous materials	315
8.2.1.	Mesoporous silica thin films obtained by self-assembly: <i>ex situ</i> and <i>in situ</i> studies	315
8.2.2.	Low- k and ultralow- k nanoporous dielectric films	317
8.2.3.	Porosity in thin films prepared by chemical routes in solution	319
8.3.	Block copolymers thin films	320
8.3.1.	Ordering of block copolymers thin films	320
8.3.2.	Phase transition of block copolymer thin films	321
8.3.3.	Dewetting of polymer thin films	322
8.4.	Thermal stability and reactivity of supported clusters	323
8.5.	<i>Ex situ</i> GISAXS studies of semi-conductor nanostructures	324
8.5.1.	Introduction	324
8.5.2.	Self-assembled Si ₃ Ge ₂ islands	324
8.5.3.	Other self-assembled semi-conductor quantum dots	326
8.5.4.	GISAXS analysis of vertical stacking of semi-conductor quantum dots	327
8.5.5.	Characterization of defects induced by implantation in semi-conductors	330
8.5.6.	Porous materials	333
8.5.7.	GISAXS studies of semi-conductor nanocrystals	333
8.5.8.	Other GISAXS studies of semi-conductors	334
8.5.9.	The use of q_x and q_y in plane directions to distinguish long-range and short-range order: The case of bonded Si wafers	334
9.	<i>In situ</i> GISAXS measurements in ultra-high vacuum, during growth	336
9.1.	3D-island growth: The metal/oxide interfaces case	336
9.1.1.	Motivations	336
9.1.2.	Investigated systems	336
9.1.3.	Preparation of samples	337
9.1.4.	General trends during growth and coalescence of islands	337
9.1.5.	Evolution of morphological parameters with thickness: Nucleation, growth and coalescence	340
9.1.6.	Information on growth modes	342
9.1.7.	Equilibrium shape, Wulff-Kaischew construction and adhesion energy	343
9.2.	Looking by GISAXS at nanoparticles during a catalytic reaction	344
9.2.1.	Scientific background: Bridging the pressure gap in surface science	344
9.2.2.	<i>In operando</i> study of gold nanoparticles on TiO ₂ (110)	344
9.3.	Stranski-Krastanow growth in the Ge/Si(001) system	345
9.4.	Self-organized growth of nanostructures	350
9.4.1.	The ordered growth of Co on Au(111)	350
9.4.2.	The ordered growth of Co on a kinked vicinal surface of Au(111)	355
9.4.3.	Self-organized growth of Co on a misfit dislocation network Ag/MgO(001)	359
9.4.4.	Self-organized growth of Ni clusters on a cobalt-oxide thin film induced by a buried misfit dislocation network	362
9.5.	Surface nanofacetting: The case of Pt on W(111)	364
9.5.1.	Nucleation and growth of 3-fold symmetry nanopramids	364
9.5.2.	Validity of the DWBA: GISAXS as function of the incident angle	366
9.5.3.	The growth of Co on a faceted Pt/W(211) surface	367
9.6.	Semi-conductor surfaces nanostructures induced by sputtering	368
9.7.	<i>In situ</i> studies of GaN surfaces	369

X-ray scattering at synchrotrons

High Brilliance allows for

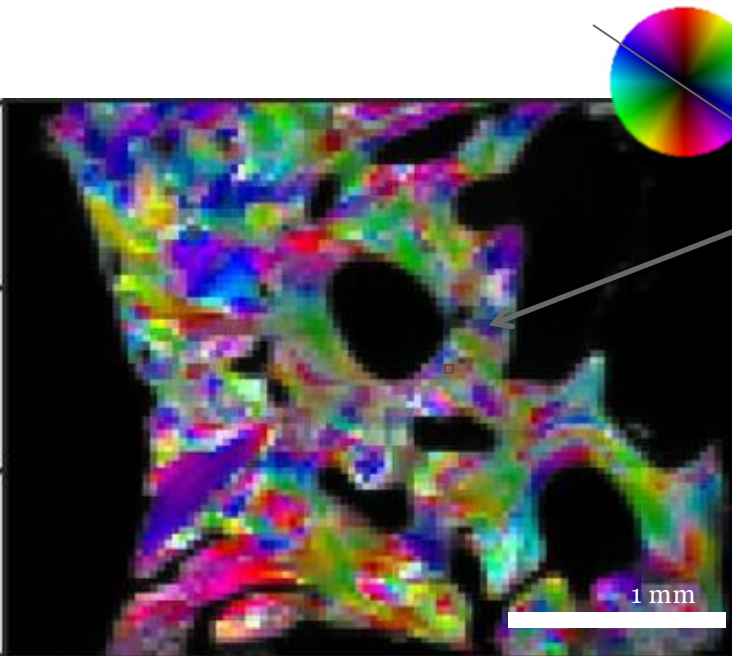
Low divergence \Rightarrow high angular resolution scattering/diffraction patterns

Tight focus \Rightarrow small sample sizes e.g., protein crystals $\sim 1 \text{ mm}^3$

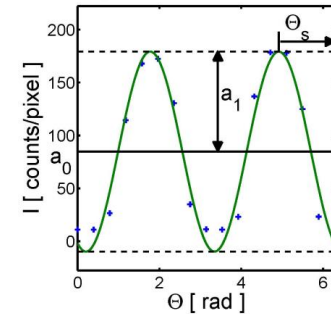
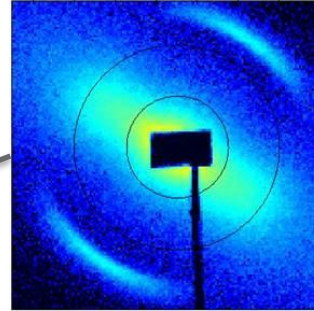
Low emittance \Rightarrow large working distance between focussing optics and sample \Rightarrow bulky sample environments

High flux \Rightarrow rapid data acquisition, time-resolved studies down to ms regime or shorter

Scanning SAXS: imaging with SAXS contrast



Hue: scattering orientation
 Saturation: degree of orientation
 Value: isotropic scattering



$$I(n_\Theta) \approx a_0 + a_1 \cos(2\pi n_\Theta / N_\Theta - \Theta_s)$$

X-ray scattering at synchrotrons

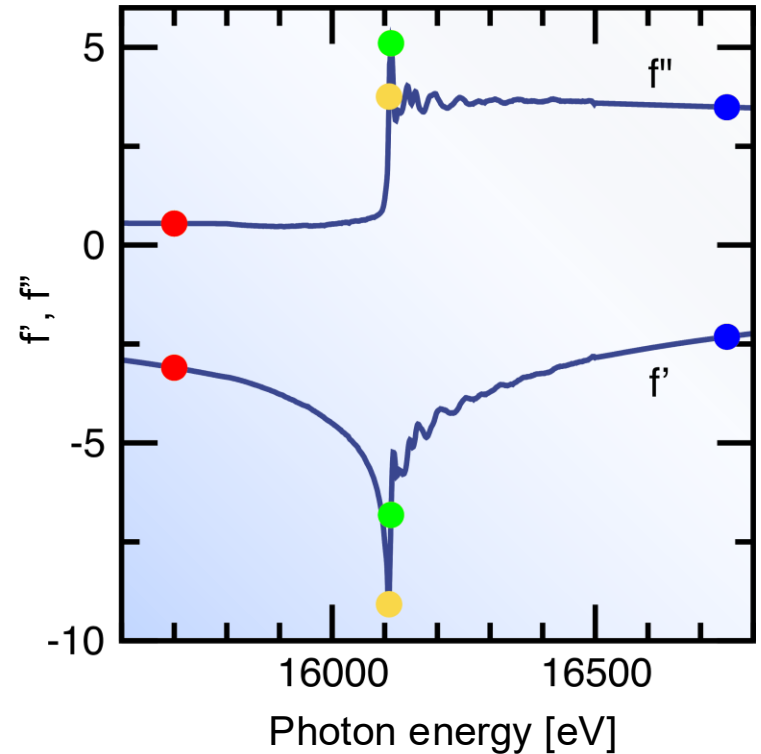
Access to high photon energies:

Penetrate deep into samples, e.g., aeronautical components, large fossils, concrete, etc.

Tunability of energy:

Abrupt changes to atomic scattering amplitudes as one crosses an absorption edge

“Anomalous” signal

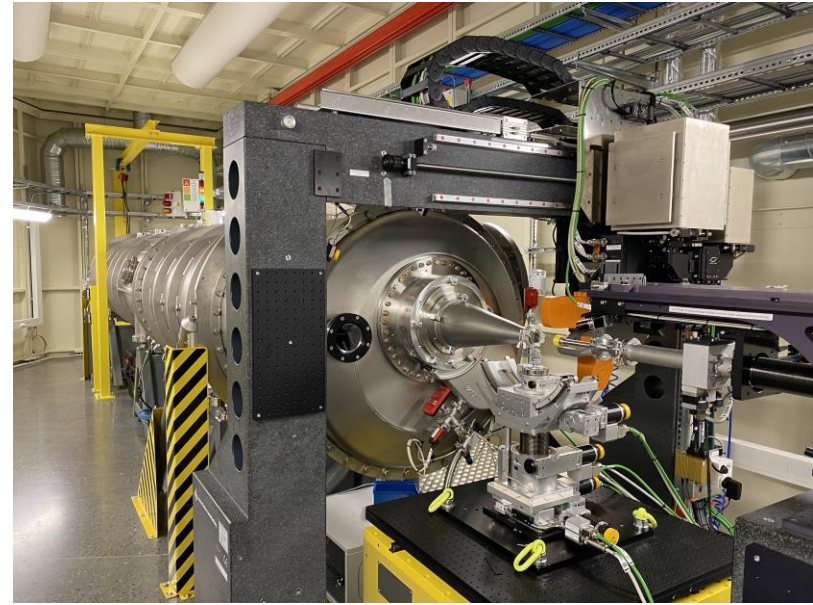


X-ray scattering at synchrotrons

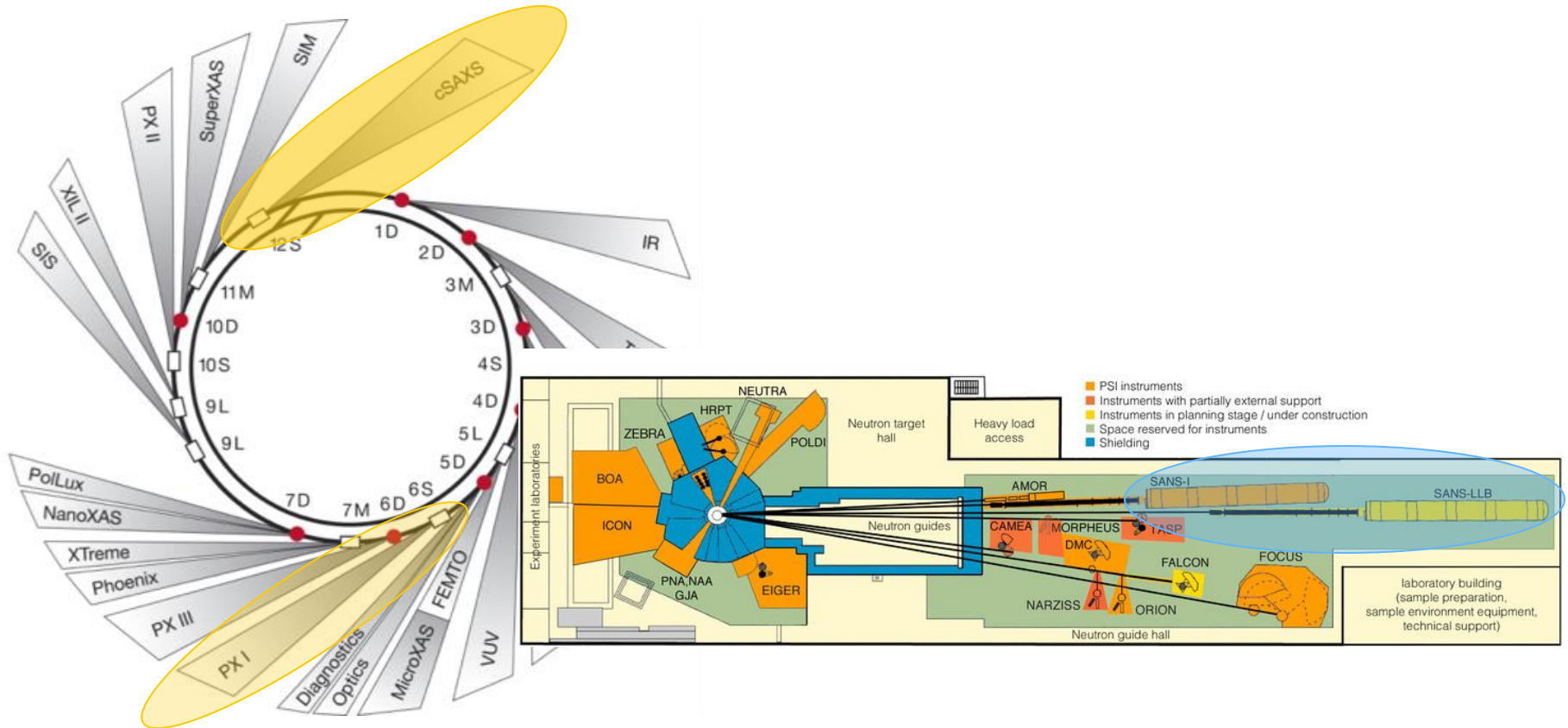
state-of-the-art detectors

shared sample environments (e.g. Rheo-SAXS)

Large flight tubes and low emittance: Ultra small angle X-ray scattering



Small angle scattering at PSI: SAXS and SANS



Practical consideration for an experiment

X-ray vs. neutrons (vs. light)

what size range is of interest \rightarrow q-range: detector distance and energy

beamsize: resolution vs. flux-density and beam damage

exposure time: signal to noise, detector speed

detector saturation

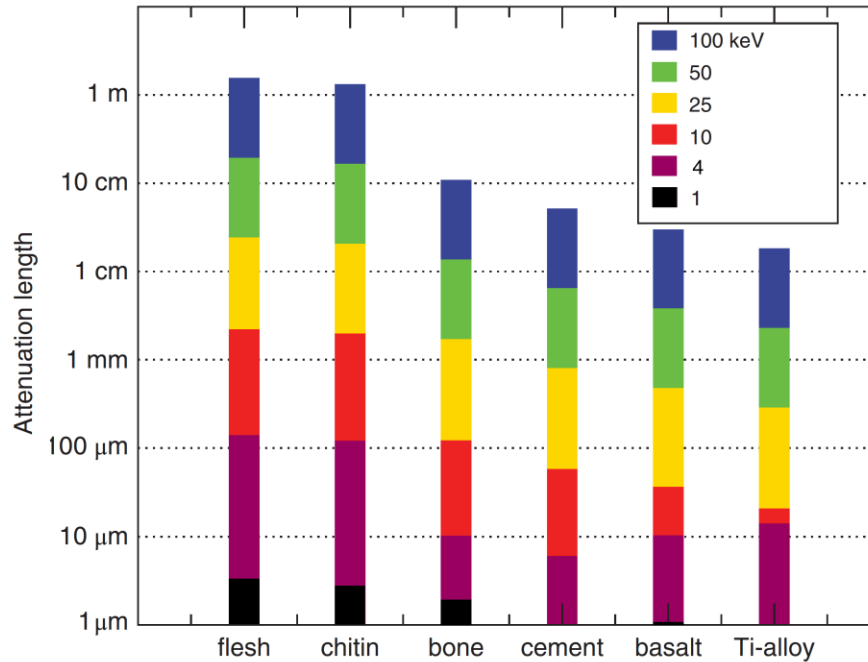
thickness of sample, for X-rays energy:

number of scatterer proportional to intensity $I(q) = (\rho_P - \rho_M)^2 N_P V_P^2 P(q) S(q)$

but absorption (Lambert-Beer law): intensity decays exponentially with thickness $I = I_0 e^{-N_i \sigma z}$

maximum at the absorption length i.e. where transmission is $1/e$, $\sim 30\%$

Sample thickness and X-ray energy



Exercise case study

You want to measure your sample with SAXS for that you need to

- choose the beamline
- define X-ray energy and sample-to-detector distance

- what size (range) do you need to probe? → define q-range
- energy depends on sample transmission and thickness → use online calculator
 - check with 1mm and 10 μm sample thickness
- chose a beamline which covers the energy range you need
- what is the minimum distance you need to place your detector for measuring your relevant size, when you have a 1mm beamstop blocking the direct beam, mounted 1cm in front of the detector
- what is the maximum q you will reach at this position considering the detector area available?

some SAXS beamline specifics (from beamline webpages)

- cSAXS@SLS
 - 4.4 – 17.9 keV
 - Pilatus 2M, pixel size 172 μm x 172 μm , active area: 254 x 289 mm^2
 - 7200 m or 2100 mm
- PX-I@SLS
 - 4.4 – 17.9 keV
 - EIGER X 16M, pixel size: 75 μm x 75 μm , active area: 311.1 x 327.2
 - max 2000 mm
- P62@DESY
 - 3.5 keV - 35.0 keV
 - Eiger2 X 9M (in vacuum), pixel size: 75 μm x 75 μm , active area: 233.1 mm x 244.7 mm
 - 1.5m up to 12.0m
- ForMAX@MAXIV
 - 8-25 keV
 - EIGER2 X 4M, pixel size: 75 μm x 75 μm , active area: 155.1 mm x 162.2 mm
 - detector distance. 800 – 7600 mm

C) Experimental method(s), specific requirements.

The proposed experiment plans to measure simultaneous scanning SAXS/WAXS with a beamsize of $25\mu\text{m}$ and a photon energy of 12.4 keV. We aim to measure samples extracted from the inferior and superior sides of each femoral neck, yielding a dataset of 180 samples in total. In order to obtain the full characterization of bone scattering parameters, we need a q -range of $0.02 - 2 \text{ nm}^{-1}$ in the SAXS regime in order to capture the collagen equatorial scattering and sufficient mineral scattering, as well as a WAXS q -range of $10-40 \text{ nm}^{-1}$ in the aim of obtaining the hydroxyapatite 002 peak ($\sim 18.2 \text{ nm}^{-1}$) in the full azimuthal range. Previous experiments at the beamline have proven the feasibility of the suggested setup in using sample-to-detector distances of 7m and 130mm for the SAXS and WAXS respectively.

